

1 **Quantifying the role of moss in terrestrial ecosystem carbon dynamics in**
2 **northern high-latitudes**

3 Junrong Zha and Qianlai Zhuang

4 Department of Earth, Atmospheric, and Planetary Sciences and Department of Agronomy,
5 Purdue University, West Lafayette, IN 47907, USA

6 Correspondence: Qianlai Zhuang (qzhuang@purdue.edu)

7 To be submitted to: *Journal of Biogeoscience*

8 **Key words: moss, carbon dynamics, Earth System Modeling, terrestrial ecosystems, Arctic**

9

10

11

12

13

14

15

16

17

18

19 Abstract

20 ~~In addition to woody and herbaceous plants, M~~mosses are ubiquitous in northern
21 terrestrial ecosystems, ~~and which~~ play an important role in regional carbon, water and
22 energy cycling. Current global land surface models that do not considering mosses may
23 bias the quantification of ~~the~~ regional carbon dynamics. ~~Here we incorporate moss into a~~
24 ~~process-based biogeochemistry model, the Terrestrial Ecosystem Model (TEM 5.0), as a~~
25 ~~new plant functional type to develop a new model (TEM_Moss). Here we incorporate~~
26 mosses as a new plant functional type into the process-based Terrestrial Ecosystem Model
27 (TEM 5.0), to develop a new model (TEM_Moss). The new model explicitly quantifies the
28 interactions between vascular plants and mosses and their competition for energy, water,
29 and nutrients. Compared to the estimates using TEM 5.0, the new model estimates that the
30 regional terrestrial soils currently store 132.7 Pg more C ~~at present day~~, and will store
31 157.5 Pg and 179.1 Pg more C under the RCP 8.5 and RCP 2.6 scenarios, respectively, by
32 the end of the 21st century. Ensemble regional simulations forced with different parameters
33 for the 21st century with TEM_Moss predict that the region will accumulate 161.1±142.1 Pg
34 C under the RCP 2.6 scenario, and 186.7±166.1 Pg C under the RCP 8.5 scenario over the
35 century. Our study highlights the necessity of coupling moss into Earth System Models to
36 adequately quantify terrestrial carbon-climate feedbacks in the Arctic.

37

38

39

40

41

42 **1. Introduction**

43 Northern high latitude ecosystems, which refers to the land ecosystems (>45 °N) in
44 northern temperate, boreal, grassland and tundra regions, hold about 30% of global terrestrial
45 carbon (C) in soils and plants (Allison and Treseder, 2008; Jobbágy and Jackson, 2000;
46 Kasischke, 2000; Tarnocai et al., 2009; Hugelius et al., 2014), and contain as much as 1024 Pg
47 soil organic carbon from 0 to 3 m depth (Treseder et al., 2016; Schuur et al., 2008). This large
48 amount of carbon is potentially responsive to ongoing global warming (Burke et al., 2017,
49 Koven et al., 2015, Comyn-Platt et al., 2018)), which is especially pronounced at high latitudes
50 (Treseder et al., 2016; IPCC, 2014). Thus, explicit investigation of carbon-climate feedback is
51 important (Wieder et al., 2013; Bond-Lamberty and Thomson, 2010).

52 Ecosystem models are important tools for understanding the role of boreal ecosystems in
53 carbon-climate feedbacks (Bond-Lamberty et al., 2005; Chadburn et al., 2017; Zhuang et al.,
54 2002; Treseder et al., 2016). Process-based biogeochemical models such as TEM (Hayes et al.,
55 2014; Raich et al., 1991; Melillo et al., 1993; McGuire et al., 1992; Zhuang et al., 2001, 2002,
56 2010, 2013), Biome-BGC (Running and Coughlan, 1988; Bond-Lamberty et al., 2007), and
57 Biosphere Energy Transfer Hydrology scheme (BETHY) (Knorr, 2000) are increasingly
58 employed to simulate current and future carbon dynamics. Those models estimate carbon
59 dynamics by simulating processes such as photosynthesis, respiration, nitrogen competition,
60 evapotranspiration and soil decomposition (Bond-Lamberty et al., 2005; Zhuang et al., 2015).
61 The results from these models are influenced by components and processes that are built into the
62 model (Turetsky et al., 2012; Oreskes et al., 1994). However, the role of boreal forests in carbon

63 sink or source activities has not yet reached a consensus due to a number of model limitations
64 (Cahoon et al., 2012; Hayes et al., 2011; Todd-Brown et al., 2013).

65 One limitation is that ecosystems models often ignore some important components such
66 as understory processes that play crucial roles in biogeochemical cycles (Zhuang et al., 2002;
67 Treseder et al., 2011; Bond-Lamberty et al., 2005). For instance, mosses are ubiquitous in
68 northern ecosystems, and show a pattern of increasing abundance with increasing latitude
69 (Turetsky et al., 2012; Jägerbrand et al., 2006). Their functional traits, including tolerance to
70 drought and a broad response of net assimilation rates to temperature, allow them to persist in
71 high-latitude regions (Kallio and Heinonen, 1975; Harley et al., 1989). The activities of moss
72 that are related to water, nutrients, and energy may influence several ecosystem processes such
73 as permafrost formation and thaw, peat accumulation, soil decomposition and net primary
74 productivity (NPP) (Turetsky et al., 2012; Nilsson and Wardle, 2005). Mosses can have positive
75 or negative interactions with vascular plants (Skre and Oechel, 1979; Turetsky et al., 2010). On
76 the one hand, mosses compete with vascular plants for available nutrients, negatively affecting
77 vascular plants productivity (Skre and Oechel, 1979; Gornall et al., 2011; Turetsky et al., 2012).
78 Besides, a thick moss cover can form an environment with water logging or low oxygen supply,
79 which is common in high-latitude regions (Skre and Oechel, 1979; Cornelissen et al., 2007). The
80 moss cover prevents absorbed solar heat from being conducted down into the soil, and tends to
81 decrease soil temperature in summer. Therefore, soil decomposition rates can be affected since
82 they are mediated by soil temperature, which will further influence growth of vascular plants
83 (Gornall et al., 2007). On the other hand, some species of mosses can serve as an important
84 source of nitrogen because of their associations with microbial nitrogen fixers (Basilier, 1979;
85 DeLuca et al., 2007; Markham, 2009; Kip et al., 2011). Thus, mosses can also exert positive

86 effects on plant growth due to their regulation of nitrogen availability for vascular plants (Hobbie
87 et al., 2000; Gornall et al., 2007). It is gradually being recognized that mosses can have
88 comparable influences on high-latitude ecosystems to vascular plants, due to their large density
89 and essential function in plant competition, soil climate, and carbon and nutrient cycling
90 (Longton, 1988; Lindo and Gonzalez, 2010; Okland, 1995; Pharo and Zartman, 2007). They can
91 on average contribute 20% of aboveground NPP in boreal forests (Turetsky et al., 2010), and
92 their annual NPP may reach as high as 350 g C m⁻² in some regions in the Arctic (Pakarinen and
93 Vitt 1973), even exceeding that of vascular plants (Oechel and Collins, 1976; Clarke et al.,
94 1971). Thus, ignorance of mosses, the keystone species of boreal ecosystems, can pose large
95 biases in model predictions and limit the utility of models. To date, a number of ecosystem
96 models have already included moss activities to explore the response of moss to disturbance
97 (Bond-Lamberty et al., 2007; Euskirchen et al., 2009; Frohking et al., 2010, Wania et al., 2009,
98 Chadburn et al., 2015, Porada et al., 2016, Druel et al., 2017), or improve model prediction of
99 carbon dynamics (Bond-Lamberty et al., 2005). However, the potential role of moss in the
100 regional carbon dynamics in northern high latitudes has been slowly evaluated by considering
101 the interactions between moss and vascular plants, especially with respect to their competition
102 for water, nutrient and energy.

103 This study developed a new version of Terrestrial Ecosystem Model (Raich et al., 1991;
104 McGuire et al., 1992; Zhuang et al., 2001, 2002, 2010, 2013, 2015), hereafter referred to as
105 TEM_Moss, by explicitly considering moss impacts on terrestrial ecosystem carbon dynamics.
106 The competition of water, energy and nutrient between vascular plants and mosses are explicitly
107 modeled. The verified TEM_Moss and previous TEM were compared against the observed data of
108 ecosystem carbon, soil temperature and moisture dynamics. Both models were then used to analyze

109 the regional carbon dynamics in northern high latitudes (north of 45 °N) during the 20th and 21st
110 centuries.

111 **2. Methods**

112 **2.1 Overview**

113 First, we briefly describe how we developed the TEM_Moss by modifying the previous
114 TEM 5.0 to consider their interactions between vascular plants and mosses. Second,
115 parameterization and validation of TEM_Moss using measured gap-filled carbon flux data and
116 meteorological data at representative sites is presented. Third, we present how we have applied
117 both models (TEM_Moss and TEM 5.0) to the northern high latitudes (above 45 °N) to quantify
118 regional carbon dynamics during the 20th and 21st centuries.

119 **2.2 Model description**

120 TEM is a process-based, large-scale biogeochemical model that uses monthly climatic data
121 and spatially explicit vegetation and soil information to simulate the dynamics of carbon and
122 nitrogen fluxes and pool sizes of plants and soils (Raich et al., 1991; McGuire et al., 1992; Zhuang
123 et al., 2010, 2015, 2020). However, in previous versions of TEM, the interactions between mosses
124 and vascular plants on carbon and nitrogen cycling have not been included. Here we developed a
125 TEM_Moss model by modifying model structure and incorporating activities of moss into extant
126 TEM 5.0 (Zhuang et al., 2003). Based on the structure of TEM 5.0, we added carbon and nitrogen
127 pools and fluxes to simulate activities of moss including photosynthesis, respiration, litterfall and
128 nutrient and water cycling (Figure 1). Thus, the structure of TEM_Moss includes the processes of
129 both vascular plants and mosses (Figure 1).

130 In TEM_Moss, moss photosynthesis (GPP_m) is described as a maximum rate, reduced by
 131 influence of photosynthetically active radiation, mean air temperature, mean atmospheric carbon
 132 dioxide concentrations, moss moisture, and indirectly, nitrogen availability (Frolking et al., 1996;
 133 Launiainen et al., 2015; Zhuang et al., 2002). For each time step, GPP_m is calculated as:

$$134 \quad GPP_m = C_{max} * f(PAR) * f(T) * f(w_m) * f([CO_2]) * f(NA) \quad (1)$$

135 where C_{max} denotes the maximum rate of carbon assimilation by moss (units: $g_C m^{-2} mon^{-1}$),
 136 $f(PAR)$ is a scalar function that depends on monthly photosynthetically active radiation (PAR),
 137 which is calculated as (Frolking et al., 1996; Launiainen et al., 2015; Kulmala et al., 2011):

$$138 \quad f(PAR) = \frac{PAR}{b+PAR} \quad (2)$$

139 where b (units: $\mu mol m^{-2} s^{-1}$) is the half saturation constant for PAR use by moss as indicated by
 140 the Michaelis–Menten kinetic.

141 The temperature effect on moss photosynthesis is modeled as a multiplier (Frolking et al.,
 142 1996; Raich et al., 1991):

$$143 \quad f(T) = \frac{(T-T_{min})*(T-T_{max})}{(T-T_{min})*(T-T_{max})-(T-T_{opt})^2} \quad (3)$$

144 where T is the monthly mean air temperature (units: $^{\circ}C$), and T_{min} , T_{max} , and T_{opt} are parameters
 145 (units: $^{\circ}C$) that limit $f(T)$ to a range of zero to one.

146 The moisture effect is also modeled as a multiplier (Frolking et al., 1996; Raich et al.,
 147 1991):

$$148 \quad f(w_m) = \frac{(w_m-w_{min})*(w_m-w_{max})}{(w_m-w_{min})*(w_m-w_{max})-(w_m-w_{opt})^2} \quad (4)$$

149 where w_m is moss moisture (units: mm), and w_{min} , w_{max} , and w_{opt} are related parameters (units:
150 mm) that limit $f(w_m)$ to a range of zero to one.

151 $f([CO_2])$ is also a scalar function that depends on monthly mean atmospheric carbon
152 dioxide concentration (Zhuang et al., 2002; Raich et al., 1991):

$$153 \quad f([CO_2]) = \frac{[CO_2]}{k_m + [CO_2]} \quad (5)$$

154 where $[CO_2]$ (units: $\mu L/L$) represents monthly mean atmospheric carbon dioxide concentration,
155 the k_m (units: $\mu L/L$) is the internal CO_2 concentration at which moss C assimilation proceeds at
156 one-half its maximum rate.

157 The function $f(NA)$ models the limiting effects of plant nitrogen status on GPP (McGuire
158 et al., 1992; Zhuang et al., 2002), which is a scalar function that depends on monthly N available
159 for incorporation into plant production of new tissue.

160 Meanwhile, in TEM_Moss, we defined the moss respiration rate (R_m) as a function of
161 moss respiration rate at 10 °C, moss respiration temperature sensitivity which was expressed as a
162 Q_{10} function, and moss moisture (Launiainen et al., 2015; Frolking et al., 1996):

$$163 \quad R_m = R_{10,m} * Q_{10,m}^{\frac{T_m - 10}{10}} * f^*(w_m) \quad (6)$$

164 where $R_{10,m}$ (units: $g_C m^{-2} mon^{-1}$) represents the moss respiration rate at 10 °C, the parameter
165 $Q_{10,m}$ is moss respiration temperature sensitivity, T_m is moss temperature (°C) and w_m is moss
166 moisture (mm).

167 The function $f^*(w_m)$ denotes the moisture effect on moss respiration. Here we used
168 $f^*(w_m)$ to distinguish with the function $f(w_m)$, which is moisture effect on moss

169 photosynthesis as mentioned earlier. $f^*(w_m)$ is defined as (Frolking et al., 1996; Zhuang et al,
 170 2002):

$$171 \quad f^*(w_m) = 1 - \frac{(w_m - w_{\min} - w_{\text{opt},r})^2}{(w_m - w_{\min}) * w_{\text{opt},r} + w_{\text{opt},r}^2} \quad (7)$$

172 where $w_{\text{opt},r}$ (units: mm) denotes the optimal water content for moss respiration.

173 Besides, the carbon in litter production from mosses to soil ($L_{C,m}$) is modeled as
 174 proportional to moss carbon biomass with a constant ratio (Zhuang et al., 2002):

$$175 \quad L_{C,m} = c_{\text{fall}_m} * \text{MOSSC} \quad (8)$$

176 where MOSSC denotes the moss carbon biomass, and c_{fall_m} is the corresponding constant
 177 proportion.

178 Thus, the change of moss carbon pool (MOSSC) can be modeled as:

$$179 \quad \frac{d\text{MOSSC}}{dt} = \text{GPP}_m - R_m - L_{C,m} \quad (9)$$

180 On the other hand, researches have shown that mosses can uptake substantial inorganic
 181 nitrogen from the bulk soil (Ayres et al., 2006, Fritz et al., 2014). In our model, nitrogen uptake
 182 by moss (N_{uptake_m}) is modelled as a function of available soil nitrogen, moss moisture, and
 183 mean air temperature, and the relative amount of energy allocated to N versus C uptake (Zhuang
 184 et al., 2002; Raich et al., 1991):

$$185 \quad N_{\text{uptake}_m} = N_{\text{max}} * \frac{K_s * N_{\text{av}}}{k_n + K_s * N_{\text{av}}} * e^{0.0693T} * (1 - A_m) \quad (10)$$

186 Where N_{max} is the maximum rate of nitrogen uptake by mosses (units: $\text{g C m}^{-2} \text{mon}^{-1}$), and N_{av}
 187 (units: g m^{-2}) represents available soil nitrogen, which is treated as a state variable in our model.

188 k_n (units: g m^{-2}) is the concentration of available soil nitrogen at which nitrogen uptake proceeds
 189 at one-half its maximum rate. T is the monthly mean air temperature ($^{\circ}\text{C}$), and A_m is a unitless
 190 parameter ranging from 0 to 1, which represents relative allocation of effort to carbon vs.
 191 nitrogen uptake. K_s is a parameter accounting for relative differences in the conductance of the
 192 soil to N diffusion, which can be calculated through moss moisture (Zhuang et al., 2002; Raich et
 193 al., 1991):

$$194 \quad K_s = 0.9 * \left(\frac{w_m}{w_f}\right)^3 + 0.1 \quad (11)$$

195 where w_f (units: mm) denotes the moss field capacity.

196 The nitrogen in litter production from mosses to soil ($L_{N,m}$) is modeled as proportional to
 197 moss nitrogen biomass with a constant ratio (Zhuang et al., 2002):

$$198 \quad L_{N,m} = nfall_m * MOSSN \quad (12)$$

199 where $nfall_m$ is the constant proportion to moss nitrogen biomass (MOSSN).

200 Thus, the changes in moss nitrogen pool (MOSSN) can be modeled as:

$$201 \quad \frac{dMOSSN}{dt} = Nuptake_m - L_{N,m} \quad (13)$$

202 At the same time, total carbon and nitrogen in litterfall, and total nitrogen uptake from
 203 soil available nitrogen are changed due to incorporation of mosses:

$$204 \quad Litterfall_C = L_{C,v} + L_{C,m} \quad (14)$$

$$205 \quad Litterfall_N = L_{N,v} + L_{N,m} \quad (15)$$

$$206 \quad Nuptake = Nuptake_v + Nuptake_m \quad (16)$$

207 Where $L_{C,v}$ and $L_{N,v}$ are carbon and nitrogen in litter production from vascular plants to soil, and
208 N_{uptake_v} is nitrogen uptake by vascular plants (Raich et al., 1991; Melillo et al., 1993; Zhuang
209 et al., 2003).

210 Except above equations, other governing equations in TEM 5.0 have not been changed.
211 More equations of TEM 5.0 have been documented in previous studies (Raich et al., 1991;
212 McGuire et al., 1992; Zhuang et al., 2003; Zha and Zhuang, 2018).

213 In TEM 5.0, a soil thermal module (STM) simulates soil thermal dynamics considering
214 the effects of moss thickness, soil moisture, and snowpack (Zhuang et al., 2001, 2002). In STM,
215 soil profile was treated as a three soil-layer system: (1) a moss plus fibric soil organic layer, (2) a
216 humic organic soil layer, and (3) a mineral soil layer, and temperature for each layer can be
217 derived from STM (Zhuang et al., 2001, 2002, 2003). Temperature in moss layer is estimated
218 with STM.

219 A water balance module (WBM) was also incorporated into TEM 5.0 to simulate soil
220 hydrologic dynamics (Vörösmarty et al., 1989; Zhuang et al., 2001). The WBM receives
221 information on precipitation, air temperature, potential evapotranspiration, vegetation, soils and
222 elevation to predict soil moisture evapotranspiration and runoff (Vörösmarty et al., 1989). The
223 whole soil was treated as a single profile in WBM (Vörösmarty et al., 1989; Zhuang et al., 2001).
224 To simulate moss moisture, we added a moss layer on the soil profile by modifying the WBM
225 (Figure 2). Similar to soil moisture, moss moisture is also treated as a state variable in the revised
226 WBM, which is modeled as:

$$227 \quad \frac{dw_m}{dt} = \text{snowfall} + \text{rainfall} - \text{percolation} - \text{moss evapotranspiration} \quad (17)$$

228 where the term “percolation” denotes the percolation from moss, which is the sum of rainfall
229 percolation and snowmelt percolation from moss. We assume that there is no runoff from moss
230 layer.

231 Accompanied by the above equation, changes in soil water (SM) is modified as:

$$232 \quad \frac{dSM}{dt} = \text{percolation} - \text{rain excess} - \text{snow excess} - \text{plant evapotranspiration} \quad (18)$$

233 Calculations for these water fluxes regarding vascular plants were not changed. More details
234 about an earlier version of WBM were described in Vörösmarty et al. (1989) and Zhuang et al.
235 (2001).

236 **2.3 Model parameterization and validation**

237 The newly introduced parameters that are associated with moss activities were documented
238 in Table 1. We parameterized the TEM_Moss for six representative ecosystem types in northern
239 high latitudes with gap-filled monthly net ecosystem productivity (NEP, $\text{g_Cm}^{-2}\text{mon}^{-1}$) data from
240 the AmeriFlux network (Davidson et al., 2000). We assumed that the moss types are associated
241 with the representative ecosystem types, which means we tuned the moss-related parameters for
242 the six representative ecosystem types. Except for the moss-related parameters, other parameters
243 related to vascular plants are default based on Zha and Zhuang, 2018. The information of six sites
244 that we chose to calibrate the TEM_Moss was compiled in Table 2. The parameterization was
245 conducted using a global optimization algorithm known as SCE-UA (Shuffled complex evolution)
246 method, which aims to minimize the difference between model simulations and measurements
247 (Duan et al., 1994). In our calibration, the cost function of the minimization is:

$$248 \quad \text{Obj} = \sum_{i=1}^k (\text{NEP}_{\text{obs},i} - \text{NEP}_{\text{sim},i})^2 \quad (19)$$

249 Where $NEP_{obs,i}$ and $NEP_{sim,i}$ are the measured and simulated NEP, respectively. k is the number
250 of data pairs for comparison. Fifty independent sets of parameters were converged to minimize the
251 objective function, and finally the optimized parameters were derived as the mean of these 50 sets
252 of inversed parameters. We presented the boxplot of parameter posterior distributions at sites
253 chosen for calibration (Figure 5). At the same time, the results of model parameterization were
254 shown in Figure 3. Besides these parameters related to moss, all other parameters use their default
255 values in TEM 5.0 (Zhuang et al., 2003). Note, in TEM 5.0 and its application, the parameters
256 were also calibrated for each representative ecosystem in northern high latitudes. Specifically,
257 TEM 5.0 was parameterized for mixed grassland/sub-shrublands, moist non-acidic tundra, mixed
258 hardwood and conifer forests, tallgrass prairie, savanna tropical forests, tussock tundra, and conifer
259 forest in the region. TEM 5.0 was then extrapolated to the region to quantify carbon dynamics
260 without considering the role of moss in boreal ecosystems (Zhuang et al., 2003). Here our revised
261 model TEM_Moss was parameterized for representative ecosystems in the region by explicitly
262 considering the role of moss in soil physics and carbon and nitrogen dynamics. The TEM_Moss
263 optimized parameters were then used for model validation and extrapolation as well as comparison
264 with TEM 5.0 simulations.

265 We verified the TEM_Moss simulated NEP, soil moisture and soil temperature. First, we
266 conducted site-level simulations at six sites that contain level-4 gap-filled monthly NEP data from
267 the AmeriFlux network (Table 3). Site-level monthly gap-filled soil moisture and soil temperature
268 data were organized from the ORNL DAAC Dataset (<https://daac.ornl.gov/>) to make comparison
269 with model simulations (Table 4 and Table 5). Local climate data including monthly air
270 temperature ($^{\circ}C$), precipitation (mm), and cloudiness (%) were obtained to drive these model
271 simulations.

272 **2.4 Regional Extrapolation**

273 With six site-level calibrated parameters, TEM-Moss is applied to the region pixel by pixel based
274 on vegetation distribution data. Both TEM_Moss and TEM 5.0 were applied to northern high
275 latitudes (above 45 °N) for historical (the 20th century) and future (the 21st century) quantifications
276 on carbon dynamics. For historical simulations, climatic forcing data including monthly air
277 temperature, precipitation, and cloudiness and atmospheric CO₂ concentrations during the 20th
278 century, were collected from the Climatic Research Unit (CRU TS3.1) from the University of East
279 Anglia (Harris et al., 2014). Other ancillary inputs including gridded soil texture (Zhuang et al.,
280 2015), elevation (Zhuang et al., 2015), and potential natural vegetation (Melillo et al., 1993) were
281 also organized. For future simulations, two contrasting Intergovernmental Panel on Climate
282 Change (IPCC) climate scenarios (RCP 2.6 and RCP 8.5) were used to drive the models. The future
283 climate forcing data and atmospheric CO₂ concentrations during the 21st century under these two
284 climate change scenarios were derived from the HadGEM2-ESmodel, which is a member of
285 CMIP5project213 (<https://esgf-node.llnl.gov/search/cmip5/>, January 2017).

286 Simulations were conducted at a spatial resolution of 0.5° latitude × 0.5° longitude (Zhuang
287 et al., 2001, 2002). A spin-up was run to reach an equilibrium for each pixel, and the values of state
288 variables at equilibrium were treated as initial values for transient simulations (McGuire et al.,
289 1992). Specifically, we chose the first 30 years in the whole 100-year climatic forcing data to spin-
290 up the models when conducting historical and future simulations. For each of the simulations, net
291 primary production (NPP), heterotrophic respiration (R_H), and net ecosystem production (NEP)
292 were analyzed. We denoted that a positive NEP represents a CO₂ sink from the atmosphere to
293 terrestrial ecosystems, while a negative value represents a source of CO₂ from terrestrial
294 ecosystems to the atmosphere.

295 In these simulations, for each pixel, we assumed its moss distribution area is the same as
296 the vascular plant distribution. The total carbon uptake/emission of mosses in a pixel are calculated
297 as the multiplication of pixel area with the carbon fluxes such as NEP (units: $\text{g}_C \text{ m}^{-2} \text{ month}^{-1}$).
298 Moss-related parameters for representative ecosystems are calibrated (Fig. 4 and Table 1) or
299 obtained from previous model parameterization and the rest of model parameters are default from
300 Zha and Zhuang (2018).

301 **3. Results**

302 **3.1 Model Validation**

303 TEM_Moss was able to reproduce the monthly NEP and performed better than TEM 5.0
304 at chosen sites, with larger R-square values and smaller RMSE (Figure 6, Table 6). R-square for
305 TEM_Moss reached 0.94 at Bartlett Experimental Forest site and 0.72 at Ivotuk site (Table 6). R-
306 square values for TEM 5.0 showed a similar pattern, reaching 0.91 and with minimum value of
307 0.43 at Bartlett Experimental Forest and Ivotuk sites, respectively (Table 6). Except for Ivotuk
308 site, R-squares for TEM_Moss are all higher than 0.8 at the chosen sites, while most R-squares
309 for TEM 5.0 are from 0.62 to 0.75 (Table 6). On the other hand, RMSE for TEM_Moss is lower
310 than that for TEM 5.0 at each site (Table 6).

311 We presented the comparisons between measured and simulated volumetric soil moisture
312 (VSM) from TEM_Moss and TEM 5.0 (Figure 7). Statistical analysis shows that TEM_Moss
313 reproduces the soil moisture well with R-squares ranging from 0.51 at US-Bkg to 0.87 at US-Atq
314 (Table 7). R-squares for TEM_Moss are substantially higher than that for TEM 5.0 at most
315 chosen sites, except for US-Atq (Table 7). RMSE for TEM_Moss is lower than that for TEM 5.0
316 at each site (Table 7). Similarly, comparisons between measured and simulated soil temperature

317 at 5 cm depth (ST_5) from TEM_Moss and TEM 5.0 indicated that TEM_Moss can reproduce
318 the soil temperature with R-squares ranging from 0.81 at US-Ho1 to 0.91 at US-Bkg, while TEM
319 5.0 reproduces the soil temperature with R-squares ranging from 0.69 at BE-Vie to 0.89 at US-
320 Bkg (Figure 8; Table 8). Although R-squares for both models are relatively high and RMSE for
321 them are relatively low, TEM_Moss still shows higher R-squares and lower RMSE than TEM
322 5.0 (Table 8).

323 **3.2 Regional carbon dynamics during the 20th century**

324 Both TEM_Moss and TEM 5.0 were used to simulate northern high-latitude regional
325 carbon balance during the 20th century (Figure 9). Higher NEP was correlated with the
326 combination of relatively higher NPP and lower heterotrophic respiration (R_H). TEM_Moss
327 indicated that the northern high latitudes acted as a carbon sink of 221.9 Pg with an inter-annual
328 standard deviation of 0.31 Pg_C yr⁻¹ during the 20th century, which is 132.7 Pg larger than 89.2 Pg
329 simulated by TEM 5.0 (Figure 10). The simulated NEP by TEM_Moss ranges from 1.38 Pg_C yr⁻¹
330 to 3.05 Pg_C yr⁻¹, while the range by TEM 5.0 was from 0.11 Pg_C yr⁻¹ to 1.75 Pg_C yr⁻¹ (Figure
331 9). The patterns of the simulated NEP from two models were similar, both showing a general
332 increasing trend throughout the 20th century (Figure 9). By 2000, the TEM_Moss simulation
333 indicated that the northern high-latitude region stored 3.05 Pg_C yr⁻¹, which is more than twice as
334 the storage estimated by TEM 5.0 (1.33 Pg_C yr⁻¹, Figure 9). Both models indicated that carbon
335 uptake by the northern ecosystems during the second half of the 20th century was higher than the
336 first half for most part of the region, and only a small portion of the region lost carbon in last
337 century (Figure 10).

338 Simulated total NPP by TEM_Moss was 9.6 Pg_C yr⁻¹, ranging from 8.52 Pg_C yr⁻¹ to
339 10.65 Pg_C yr⁻¹ in the 20th century, with 1.69 Pg_C yr⁻¹ of moss NPP and 7.93 Pg_C yr⁻¹ of

340 vascular plants NPP (Figure 9). Moss NPP ranges from 1.23 Pg_C yr⁻¹ to 2.14 Pg_C yr⁻¹ and the
341 ratio of moss NPP to vascular plants NPP is 0.21 (Figure 9). TEM 5.0 estimated 0.8 Pg_C yr⁻¹
342 lower total NPP than TEM_Moss, but 0.87 Pg_C yr⁻¹ higher NPP for vascular plants (Figure 9).
343 On the other hand, average heterotrophic respiration in the 20th century was 7.38 Pg_C yr⁻¹ and
344 all years were within about 5% of this value (Figure 9). TEM 5.0 projected 0.53 Pg_C yr⁻¹ higher
345 R_H than TEM_Moss (7.91 Pg_C yr⁻¹, Figure 9). Overall, TEM_Moss predicted higher total NPP
346 but lower R_H, which jointly caused a pronounced difference in NEP between two models.

347 Both models estimated that soil organic carbon and vegetation carbon were accumulating
348 continuously in the 20th century (Figure 11). TEM_Moss indicated that regional SOC and VEGC
349 accumulated 96.3 Pg_C and 115.2 Pg_C, respectively, and the carbon uptake by moss was 10.4 Pg
350 in the period (Figure 11, Table 10). As simulated by TEM_Moss, 43.4%, 51.9% and 4.7% of
351 total carbon uptake in the region was assimilated to soils, vascular plants and mosses,
352 respectively (Table 10). TEM 5.0 simulated that SOC increased by 31.7 Pg at the end of the 20th
353 century, which is 64.6 Pg_C less than the value estimated by TEM_Moss (Table 10). TEM 5.0
354 estimated 57.7 Pg_C in plants less than the value estimated by TEM_Moss (57.5 Pg_C, Table 10).
355 35.5% and 64.5% of total carbon was as SOC and VEGC, respectively.

356 **3.3 Regional carbon dynamics during the 21st century**

357 Under the RCP 2.6 scenario, TEM_Moss simulated NEP of 2.07 Pg_C yr⁻¹ with the range
358 from 0.41 Pg_C yr⁻¹ to 3.2 Pg_C yr⁻¹, and the inter-annual standard deviation of 0.59 Pg_C yr⁻¹
359 during the 21st century (Figure 12 (a)). The regional sink shows a decreasing pattern in the 2000s
360 and then generally increases over the remaining years of the 21st century (Figure 12 (a)). For
361 comparison, TEM 5.0 predicted that the average NEP of 0.28 Pg_C yr⁻¹ with the range from -1.48
362 Pg_C yr⁻¹ to 1.69 Pg_C yr⁻¹ during the 21st century (Figure 12 (a)). Thus, TEM 5.0 projected 179.1

363 Pg_C stored in northern ecosystems is less than the estimation from TEM_Moss in the 21st
364 century. Besides, TEM 5.0 simulated that the regional NEP showed a decreasing trend and the
365 region fluctuates between sinks and sources during the century (Figure 12 (a)). The spatial
366 patterns from two models also showed differences. TEM_Moss indicated that the region
367 accumulates carbon over this century, while TEM 5.0 simulated that some regions changed from
368 a carbon sink to a source in the second half of the century (Figure 13 (a)). Simulated regional
369 NPP by TEM_Moss ranges from 11.2 to 13.7 Pg_C yr⁻¹ with a mean of 12.98 Pg_C yr⁻¹ in this
370 century, while average NPP predicted by TEM 5.0 is 1.46 Pg_C yr⁻¹ lower than that value (11.52
371 Pg_C yr⁻¹ (Figure 12(a)). TEM_Moss simulated NPP has 3.74 Pg_C yr⁻¹ from moss and 9.24 Pg_C
372 yr⁻¹ from vascular plants, which account for 28.8% and 71.2% of total NPP, respectively (Figure
373 12(a)). Meanwhile, TEM_Moss estimated that R_H is 10.91 Pg_C yr⁻¹, while TEM 5.0 predicted it
374 as 11.24 Pg_C yr⁻¹, which is higher (Figure 12(b)). Both models projected that soil organic carbon
375 and vegetation carbon accumulate in this century but with different magnitudes (Figure 14 (a)).
376 TEM_Moss predicted that regional SOC and VEGC accumulated 84.7 Pg_C and 112.6 Pg_C,
377 respectively, during the 21st century, while TEM 5.0 predicted that a smaller increase with 12.1
378 and 15.5 Pg_C in SOC and VEGC, respectively (Figure 14 (a), Table 12 (a)). Besides,
379 TEM_Moss also predicted an increasing of 9.4 Pg_C in MOSSC, accounting for 4.5% of the total
380 carbon uptake in this region (Table 12(a)).

381 Under the RCP 8.5 scenario, TEM_Moss simulated annual NPP of 13.84 Pg_C yr⁻¹ with a
382 range from 11.09 to 16.94 Pg_C yr⁻¹, which is 1.31 Pg_C yr⁻¹ higher than the projection from
383 TEM 5.0 (Figure 12 (b)). Total NPP estimated by TEM_Moss has 3.84 Pg_C yr⁻¹ from moss and
384 10 Pg_C yr⁻¹ from vascular plants (Figure 12(b)). Annual R_H was 11.28 Pg_C yr⁻¹ estimated by
385 TEM_Moss and 11.54 Pg_C yr⁻¹ by TEM 5.0, respectively (Figure 12(b)). Consequently,

386 TEM_Moss projected NEP was 2.56 Pg_C yr⁻¹ with the inter-annual standard deviation of 0.93
387 Pg_C yr⁻¹ in this century (Figure 12(b)). NEP ranges from 0.67 Pg_C yr⁻¹ to 4.78 Pg_C yr⁻¹
388 estimated with TEM_Moss, while from -1.69 Pg_C yr⁻¹ to 2.65 Pg_C yr⁻¹ with a mean of 0.99 Pg
389 C yr⁻¹ was estimated by TEM 5.0 (Figure 12(b)). TEM_Moss predicted more carbon uptake of
390 157.5 Pg than TEM 5.0 during the 21st century. Both models predicted that NEP showed an
391 increasing trend during the 21st century (Figure 12(b)). Moreover, similar spatial patterns of
392 carbon sinks and sources appeared in the projections from two models (Figure 13(b)). Soil
393 organic carbon and vegetation carbon shows an increasing trend from both models (Figure
394 14(b)). Regional SOC and VEGC increased by 92.5 Pg_C and 153.6 Pg_C, respectively by the
395 end of the 21st century predicted by TEM_Moss. In contrast, the increase of 44.2 Pg_C and 54.5 Pg
396 C of SOC and VEGC, respectively, was predicted by TEM 5.0 (Figure 14(b), Table 12 (b)).
397 TEM_Moss predicted an increase of 10.1 Pg_C in MOSSC (Table 12(b)).

398 **4. Discussion**

399 **4.1 The role of moss in the regional carbon dynamics**

400
401 Global warming has been pronounced in recent decades, particularly at high latitudes
402 (IPCC, 2014; Tape et al., 2006; Stow et al., 2004). An enormous amount of soil organic carbon
403 stored in northern high-latitude regions (Tarnocai et al., 2009; Schuur et al., 2008) is expected to
404 affect a broad spectrum of ecological and human systems, and cause rapid changes in the Earth
405 system when undergoing substantial climate change (Serreze and Francis 2006; Davidson and
406 Janssens, 2006; McGuire et al., 2009). Improving projections for carbon budget of high latitude
407 terrestrial ecosystems is essential for understanding global carbon–climate feedbacks (Melillo et
408 al., 2011; Todd-Brown et al., 2013).

409 Our simulations suggest that mosses play an important role in the regional carbon
410 dynamics, which is consistent with previous studies (McGuire et al., 2009; Turetsky et al., 2012).
411 First of all, mosses are productive with carbon assimilation even during low temperature, water
412 content and irradiance (Kallio and Heinonen, 1975; Harley et al., 1989). For example, mosses
413 can tolerate drought through physiological responses, such as by suspending metabolism and by
414 withstanding cell desiccation (Turetsky et al., 2012; Oechel and Van Cleve, 1986). The key
415 functional traits related to water, nutrient, and thermal tolerances of mosses enable them to fit in
416 harsh northern conditions (Shetler et al., 2008; Turetsky et al., 2012). Thus, with incorporation of
417 moss into our models, the total NPP estimation in our model is affected. Mosses also act as a
418 powerful competitor with vascular plants for nutrient uptake. Their rapid nutrient acquisition and
419 slow nutrient loss through slow decomposition may constrain concentrations of plant-available
420 nitrogen (Hobbie et al., 2000; Turetsky et al., 2010; Oechel and Van Cleve, 1986; Gornall et al.,
421 2007), which will further decrease NPP of vascular plants. Our model results suggested that the
422 NPP of vascular plants considering moss is indeed lower than previous NPP estimates without
423 considering moss, but the total NPP is larger than before. We estimated that mosses contribute
424 17.6% of NPP in the 20th century, and 28.8% and 27.6% in the 21st century under the RCP 2.6
425 and RCP 8.5 scenarios, respectively. This is comparable with the results reported by a synthesis
426 study, indicating an average contribution 20% of aboveground NPP from moss in upland boreal
427 forests and the contribution is 48% in wetlands ecosystems. Frohking et al. (1996) even reported
428 a contribution of 38.4% to total NPP by moss at a boreal forest site. Moreover, mosses can also
429 influence heterotrophic respiration (R_H) through their effects on soil thermal and hydrologic
430 dynamics (Zhuang et al., 2001). With the layer of moss, soil temperature tends to decrease but
431 soil moisture tends to increase (Oechel and Van Cleve, 1986), which will further decrease soil

432 respiration in summer. This supports our results that TEM_Moss simulated R_H is lower than that
433 by TEM 5.0. With a combination of higher NPP and lower R_H , NEP predicted by TEM_Moss is
434 larger than that by TEM 5.0. The two contrasting regional simulations by TEM_Moss and TEM
435 5.0 indicated the region is currently a carbon sink, which is consistent with previous studies
436 (White et al., 2000; McGuire et al., 2009; Schimel et al., 2001). Our study estimates that regional
437 NEP during the 20th century is 2.2 Pg C yr⁻¹ by TEM_Moss and 0.89 Pg C yr⁻¹ by TEM 5.0,
438 respectively. In the 1990s, the regional sink is projected to be 2.7 and 1.1 Pg C yr⁻¹ by
439 TEM_Moss and TEM 5.0 respectively. Compared with other existing studies, our regional
440 estimates of NEP are within the reasonable range from other existing studies. McGuire et al.
441 (2009) estimated a land sink of 0.3–0.6 Pg C yr⁻¹ for the pan-arctic region for the 1990s, which is
442 closer to our estimation by TEM 5.0 but less than the projection by TEM_Moss. The top-down
443 atmospheric analyses indicate that the sink of pan-arctic region is between 0 and 0.8 Pg C yr⁻¹ in
444 the 1990s (Menon et al. 2007). Besides, Schimel et al. (2001) reported an estimation of the
445 northern extratropical NEP is from 0.6 to 2.3 Pg C yr⁻¹ in the late 20th century, which is
446 comparable to our estimates. Our simulations also confirmed that mosses and vascular plants
447 respond to climate change similarly in terms of their productivity (Turetsky et al. 2010).

448 **4.2 Model Uncertainty and limitations**

449 There are a number of uncertainty sources in our model simulations. First, due to the
450 limited understanding of moss photosynthesis (He et al., 2015) and various moss N uptake
451 pathways (e.g., Bay et al 2013; Berg et al 2013), a few important assumptions have been made in
452 our modeling. For instance, we assume that mosses behave similarly to vascular plants regarding
453 photosynthesis and soil N uptake is the only pathway for mosses without considering N uptake
454 through N fixers and atmospheric wet N deposition (Ayres et al. 2006). Second, the errors in the

455 observed data will influence our parameterization results, which will bias our regional estimates
456 of carbon dynamics. Second, climatic driving data are also a source of uncertainty for historical
457 and future simulations. Third, model assumptions will also induce additional uncertainties. For
458 instance, we assumed that vegetation distribution will remain unchanged during the transient
459 simulation. However, vegetation will change in response to warming climate and disturbances
460 such as fire and insect outbreaks in the region (Hansen et al., 2006), which will affect carbon
461 budget. Missing potential responses to disturbances in our model shall introduce additional
462 uncertainties (Soja et al. 2007; Kasischke and Turetsky, 2006). Future moss dynamics will also
463 impact carbon dynamics in this region. For instance, a long-term warming experiments along
464 natural climatic gradients, ranging from Swedish subarctic birch forest and subarctic/subalpine
465 tundra to Alaskan arctic tussock tundra concluded that both diversity and abundance of mosses
466 are likely to decrease under arctic climate warming (Long et al. 2012). Similarly, total moss
467 cover declined in both heath and mesic meadow under experimental long-term warming (by 1.5–
468 3 °C), driven by general declines in many species (Alatalo et al., 2020). Due to global warming,
469 significant losses in moss diversity are expected in boreal forests and alpine biomes, leading to
470 changes in ecosystem structure and function, nutrient cycling, and carbon balance (He et al.,
471 2015).

472 We conducted ensemble regional simulations with 50 sets of parameters to quantify
473 model uncertainty due to uncertain parameters. The 50 sets of parameters were obtained using
474 the method in Tang and Zhuang (2008). The ensemble means and the inter-simulation standard
475 deviations are used to measure the model uncertainty (Figure 15). TEM_Moss predicted that the
476 regional cumulative carbon ranges from a carbon loss of 266 Pg C to a carbon sink of 567.3 Pg C
477 by different ensemble members, with a mean of 161.1 ± 142.1 Pg during the 21st century under the

478 RCP 2.6 scenario. Under the RCP 8.5 scenario, TEM_Moss predicted that the region acts from a
479 carbon source of 79.1 Pg C to a carbon sink of 625.9 Pg C, with a mean of 186.7 ± 166.1 Pg
480 during the 21st century (Figure 15).

481 This study took an important step to incorporate moss into an extant ecosystem model
482 that has not explicitly consider the role of moss and its interactions with vascular plants. Our
483 model simulations showed that mosses have strong influences on regional ecosystem carbon
484 cycling, by affecting the soil thermal, nitrogen availability, and water conditions of terrestrial
485 ecosystems. However, there are still limitations in our model. First, we did not differentiate
486 various kinds of mosses because they have their own functional traits. Different kinds of mosses
487 may provide different levels of insulation for soil, resulting in different soil thermal conditions
488 that affect microbial activities. The structural and physiological traits of mosses will differ
489 largely in different moss groups, such as feather moss versus Sphagnum (Turetsky et al., 2010).
490 In addition, we lack spatially explicit information of moss distribution in the region, which will
491 lead to a large regional uncertainty of carbon quantification. We assumed that moss area
492 distribution is the same as its associated vegetation distribution. Another limitation is that some
493 important physiological traits of moss have not been modeled. For example, moss abundance
494 may change following shifts in vascular species composition due to shading or burial by vascular
495 litter (Turetsky et al., 2010; Cornelissen et al., 2007). Furthermore, disturbance such as wildfires
496 can also influence moss activities.

497 **5. Conclusions**

498 This study explicitly incorporated moss into an extant process-based terrestrial ecosystem model
499 to investigate the carbon dynamics in the Arctic for present day and future. Historical regional
500 simulations with TEM_Moss indicated that the region is a carbon sink of 221.9 Pg_C over the 20th

501 century, and this sink may decrease to 206.7 Pg_C under the RCP 2.6 scenario or increase to 256.2
502 Pg_C under the RCP 8.5 scenario during the 21st century. Compared with an earlier version of TEM
503 that has not explicitly modeled moss, TEM_Moss projected that the region stored 132.7 Pg more
504 C over the last century, 179.1 Pg and 157.5 Pg more C under the RCP 2.6 and RCP 8.5 scenarios,
505 respectively. This study demonstrated that moss activities have large effects on ecosystem soil
506 thermal, water, and carbon dynamics through their interactions with vascular plants. This study
507 highlights the importance of considering the moss dynamics in Earth System Models to adequately
508 quantify the carbon–climate feedbacks in the Arctic.

509 **6. Acknowledgments**

510 This research was supported by an NSF project (IIS-1027955), a DOE project (DE-SC0008092),
511 and a NASA LCLUC project (NNX09AI26G). We acknowledge the Rosen High Performance
512 Computing Center at Purdue for computing support. We also acknowledge the World Climate
513 Research Programme’s Working Group on Coupled Modeling Intercomparison Project CMIP5,
514 and we thank the climate modeling groups for producing and making available their model
515 output. The data of this study can be accessed from Purdue Research Repository.

516

517 **References**

518 Allison, S. D., and Treseder, K. K.: Warming and drying suppress microbial activity and carbon cycling in
519 boreal forest soils, *Global change biology*, 14, 2898-2909, 10.1111/j.1365-2486.2008.01716.x, 2008.
520 Basilier, K.: Moss-associated nitrogen fixation in some mire and coniferous forest environments around
521 Uppsala, Sweden, *Lindbergia*, 5, 84-88, 1979.
522 Bay, G., Nahar, N., Oubre, M., Whitehouse, M.J., Wardle, D.A., Zackrisson, O., Nilsson, M.-C. and
523 Rasmussen, U. (2013), Boreal feather mosses secrete chemical signals to gain nitrogen. *New Phytol*, 200:
524 54-60. <https://doi.org/10.1111/nph.12403>

525 Ben Bond-Lamberty, S. T. G., Douglas E. Ahl and Peter E. Thornton: Reimplementation of the Biome-
526 BGC model to simulate successional change, *Tree Physiology*, 25, 413–424, 2005.

527 Berg, Andreas, et al. “Transfer of Fixed-N from N₂-Fixing Cyanobacteria Associated with the Moss
528 Sphagnum Riparium Results in Enhanced Growth of the Moss.” *Plant and Soil*, vol. 362, no. 1/2, 2013,
529 pp. 271–278. JSTOR, www.jstor.org/stable/42951898. Accessed 28 May 2021.

530 Bond-Lamberty, B., Peckham, S. D., Ahl, D. E., and Gower, S. T.: Fire as the dominant driver of central
531 Canadian boreal forest carbon balance, *Nature*, 450, 89-92, 10.1038/nature06272, 2007.

532 Bond-Lamberty, B., and Thomson, A.: Temperature-associated increases in the global soil respiration
533 record, *Nature*, 464, 579-582, 10.1038/nature08930, 2010.

534 Burke, E. J., Ekici, A., Huang, Y., Chadburn, S. E., Huntingford, C., Ciais, P., Friedlingstein, P., Peng, S.
535 & Krinner, G. 2017. Quantifying uncertainties of permafrost carbon-climate feedbacks. *Biogeosciences*,
536 14, 3051-3066.

537 Cahoon, S. M., Sullivan, P. F., Shaver, G. R., Welker, J. M., Post, E., and Holyoak, M.: Interactions
538 among shrub cover and the soil microclimate may determine future Arctic carbon budgets, *Ecology*
539 *letters*, 15, 1415-1422, 10.1111/j.1461-0248.2012.01865.x, 2012.

540 Chadburn, S. E., Burke, E. J., Cox, P. M., Friedlingstein, P., Hugelius, G., and Westermann, S.: An
541 observation-based constraint on permafrost loss as a function of global warming, *Nature Climate Change*,
542 7, 340-344, 10.1038/nclimate3262, 2017.

543 Charles J. Vörösmarty, B. M. I., Annette L. Grace, and M. Patricia Gildea: Continental scale models of
544 water balance and fluvial transport: an application to South America, *Global biogeochemical cycles*, 3,
545 241-265, 1989.

546 Christian Fritz, L. P. M. L., Muhammad Riaz, Leon J. L. van den Berg, Theo J. T.M. Elzenga: Sphagnum
547 Mosses - Masters of Efficient N-Uptake while Avoiding Intoxication, *PLoS ONE*, 9,
548 10.1371/journal.pone.0079991, 2014.

549 Clarke, G. C. S.: Productivity of Bryophytes in Polar Regions, *Annals of botany*, 35, 99–108, 1971.

550 Collins, W. C. O. a. N. J.: Comparative CO₂ exchange patterns in mosses from two tundra habitats at
551 Barrow, Alaska, *Canadian Journal of Botany*, 54, 1355-1369, 1976.

552 Comyn-Platt, E., Hayman, G., Huntingford, C., Chadburn, S. E., Burke, E. J., Harper, A. B., Collins, W.
553 J., Webber, C. P., Powell, T., Cox, P. M., Gedney, N. & Sitch, S. 2018. Carbon budgets for 1.5 and 2 °C
554 targets lowered by natural wetland and permafrost feedbacks. *Nature Geoscience*, 11, 568-573.

555 Cornelissen, J. H., Lang, S. I., Soudzilovskaia, N. A., and Daring, H. J.: Comparative cryptogam ecology:
556 a review of bryophyte and lichen traits that drive biogeochemistry, *Annals of botany*, 99, 987-1001,
557 10.1093/aob/mcm030, 2007.

558 Davidson, E. A., Trumbore, S. E., and Amundson, R.: Soil warming and organic carbon content, *Nature*,
559 408, 789, 10.1038/35048672, 2000.

560 Davidson, E. A., and Janssens, I. A.: Temperature sensitivity of soil carbon decomposition and feedbacks
561 to climate change, *Nature*, 440, 165-173, 10.1038/nature04514, 2006.

562 Davidson, E. A., Janssens, I. A., and Luo, Y.: On the variability of respiration in terrestrial ecosystems:
563 moving beyond Q10, *Global change biology*, 12, 154-164, 10.1111/j.1365-2486.2005.01065.x, 2006.

564 DeLuca, T. H., Zackrisson, O., Gentili, F., Sellstedt, A., and Nilsson, M. C.: Ecosystem controls on
565 nitrogen fixation in boreal feather moss communities, *Oecologia*, 152, 121-130, 10.1007/s00442-006-
566 0626-6, 2007.

567 Duan, Q., Sorooshian, S., and Gupta, V. K.: Optimal use of the SCE-UA global optimization method for
568 calibrating watershed models, *Journal of Hydrology*, 158, 265-284, 1994.

569 E. S. Euskirchen, A. D. M., F. S. Chapin, III, S. Yi, and C. C. Thompson: Changes in vegetation in
570 northern Alaska under scenarios of climate change, 2003–2100: implications for climate feedbacks,
571 *Ecological Applications*, 19, 1022–1043, 2009.

572 Edward A. G. Schuur, J. B., Josep G. Canadell, Eugenie Euskirchen, Christopher B., Field, S. V. G.,
573 Stefan Hagemann, Peter Kuhry, Peter M. Lafleur, Hanna Lee, Galina, Mazhitova, F. E. N., Annette Rinke,
574 Vladimir E. Romanovsky, Nikolay Shiklomanov, and Charles Tarnocai, S. V., Jason G. Vogel, And Sergei
575 A. Zimov: Vulnerability of Permafrost Carbon to Climate Change: Implications for the Global Carbon
576 Cycle, *BioScience*, 58, 701-714, 2008.

577 Edward Ayres, R. v. d. W., Martin Sommerkorn, Richard D. Bardgett: Direct uptake of soil nitrogen by
578 mosses, *Biology Letters*, 2, 286-288, 10.1098/rsbl.2006.0455, 2006.

579 Esteban G. Jobbágy, and Jackson, R. B.: The vertical distribution of soil organic carbon and its relation to
580 climate and vegetation, *Ecological applications*, 10, 423-436, 2000.

581 Frohking, S., Roulet, N. T., Tuittila, E., Bubier, J. L., Quillet, A., Talbot, J., and Richard, P. J. H.: A new
582 model of Holocene peatland net primary production, decomposition, water balance, and peat
583 accumulation, *Earth System Dynamics*, 1, 1-21, 10.5194/esd-1-1-2010, 2010.

584 Gilmanov, T. G., Tieszen, L. L., Wylie, B. K., Flanagan, L. B., Frank, A. B., Haferkamp, M. R., Meyers,
585 T. P., and Morgan, J. A.: Integration of CO₂ flux and remotely-sensed data for primary production and
586 ecosystem respiration analyses in the Northern Great Plains: potential for quantitative spatial
587 extrapolation, *Global Ecology and Biogeography*, 14, 271-292, 10.1111/j.1466-822X.2005.00151.x, 2005.

588 Gornall, J. L., Jonsdottir, I. S., Woodin, S. J., and Van der Wal, R.: Arctic mosses govern below-ground
589 environment and ecosystem processes, *Oecologia*, 153, 931-941, 10.1007/s00442-007-0785-0, 2007.

590 Gornall, J. L., Woodin, S. J., Jonsdottir, I. S., and van der Wal, R.: Balancing positive and negative plant
591 interactions: how mosses structure vascular plant communities, *Oecologia*, 166, 769-782,
592 10.1007/s00442-011-1911-6, 2011.

593 Gough, C. M., Hardiman, B. S., Nave, L. E., Bohrer, G., Maurer, K. D., Vogel, C. S., Nadelhoffer, K. J.,
594 and Curtis, P. S.: Sustained carbon uptake and storage following moderate disturbance in a Great Lakes
595 forest, *Ecological Applications*, 23, 1202-1215, 2013.

596 Goulden, M. L., Winston, G. C., McMillan, A. M. S., Litvak, M. E., Read, E. L., Rocha, A. V., and Rob
597 Elliot, J.: An eddy covariance mesonet to measure the effect of forest age on land atmosphere exchange,
598 *Global change biology*, 12, 2146-2162, 10.1111/j.1365-2486.2006.01251.x, 2006.

599 Hansen, J., Sato, M., Ruedy, R., Lo, K., Lea, D. W., and Medina-Elizade, M.: Global temperature change,
600 *Proceedings of the National Academy of Sciences of the United States of America*, 103, 14288-14293,
601 10.1073/pnas.0606291103, 2006.

602 Harris, I., Jones, P. D., Osborn, T. J., and Lister, D. H.: Updated high-resolution grids of monthly climatic
603 observations - the CRU TS3.10 Dataset, *International Journal of Climatology*, 34, 623-642,
604 10.1002/joc.3711, 2014.

605 Hayes, D. J., McGuire, A. D., Kicklighter, D. W., Gurney, K. R., Burnside, T. J., and Melillo, J. M.: Is the
606 northern high-latitude land-based CO₂ sink weakening?, *Global Biogeochemical Cycles*, 25, n/a-n/a,
607 10.1029/2010gb003813, 2011.

608 Hayes, D. J., Kicklighter, D. W., McGuire, A. D., Chen, M., Zhuang, Q., Yuan, F., Melillo, J. M., and
609 Wullschleger, S. D.: The impacts of recent permafrost thaw on land-atmosphere greenhouse gas
610 exchange, *Environmental Research Letters*, 9, 045005, 10.1088/1748-9326/9/4/045005, 2014.

611 Xiaolan He, Kate S. He, Jaakko Hyvönen, Will bryophytes survive in a warming world?,
612 *Perspectives in Plant Ecology, Evolution and Systematics*, Volume 19, 2016, Pages 49-60,
613 ISSN 1433-8319, <https://doi.org/10.1016/j.ppees.2016.02.005>.

614 Hiller, R. V., McFadden, J. P., and Kljun, N.: Interpreting CO₂ Fluxes Over a Suburban Lawn: The
615 Influence of Traffic Emissions, *Boundary-Layer Meteorology*, 138, 215-230, 10.1007/s10546-010-9558-
616 0, 2010.

617 Hugelius, G., Strauss, J., Zubrzycki, S., Harden, J. W., Schuur, E. A. G., Ping, C. L., Schirmer, L.,
618 Grosse, G., Michaelson, G. J., Koven, C. D., amp, apos, Donnell, J. A., Elberling, B., Mishra, U., Camill,
619 P., Yu, Z., Palmtag, J., and Kuhry, P.: Estimated stocks of circumpolar permafrost carbon with quantified
620 uncertainty ranges and identified data gaps, *Biogeosciences*, 11, 6573-6593, 10.5194/bg-11-6573-2014,
621 2014.

622 Jägerbrand, A. K., Lindblad, K. E. M., Björk, R. G., Alatalo, J. M., and Molau, U.: Bryophyte and Lichen
623 Diversity Under Simulated Environmental Change Compared with Observed Variation in Unmanipulated
624 Alpine Tundra, *Biodiversity and Conservation*, 15, 4453-4475, 10.1007/s10531-005-5098-1, 2006.

625 Jenkins, J. P., Richardson, A. D., Braswell, B. H., Ollinger, S. V., Hollinger, D. Y., and Smith, M. L.:
626 Refining light-use efficiency calculations for a deciduous forest canopy using simultaneous tower-based
627 carbon flux and radiometric measurements, *Agricultural and Forest Meteorology*, 143, 64-79,
628 10.1016/j.agrformet.2006.11.008, 2007.

629 Juha M Alatalo, Annika K Jägerbrand, Mohammad Bagher Erfanian, Shengbin Chen, Shou-Qin Sun, Ulf
630 Molau, Bryophyte cover and richness decline after 18 years of experimental warming in alpine Sweden,
631 *AoB PLANTS*, Volume 12, Issue 6, December 2020, plaa061, <https://doi.org/10.1093/aobpla/plaa061>

632 Kasischke, E. S.: Boreal ecosystems in the global carbon cycle. In *Fire, climate change, and carbon*
633 *cycling in the boreal forest*, *Ecological Studies (Analysis and Synthesis)*, 138, 19-30,
634 https://doi.org/10.1007/978-0-387-21629-4_2, 2000.

635 Kasischke, E. S., and Turetsky, M. R.: Recent changes in the fire regime across the North American
636 boreal region—Spatial and temporal patterns of burning across Canada and Alaska, *Geophysical Research*
637 *Letters*, 33, 10.1029/2006gl025677, 2006.

638 Kip, N., Ouyang, W., van Winden, J., Raghoebarsing, A., van Niftrik, L., Pol, A., Pan, Y., Bodrossy, L.,
639 van Donselaar, E. G., Reichart, G. J., Jetten, M. S., Damste, J. S., and Op den Camp, H. J.: Detection,
640 isolation, and characterization of acidophilic methanotrophs from Sphagnum mosses, *Applied and*
641 *environmental microbiology*, 77, 5643-5654, 10.1128/AEM.05017-11, 2011.

642 Knorr, W.: Annual and interannual CO₂ exchanges of the terrestrial biosphere: process-based simulations
643 and uncertainties, *Global Ecology and Biogeography*, 9, 225-252, 2000.

644 Koven, C. D., Schuur, E. A. G., Schädel, C., Bohn, T. J., Burke, E. J., Chen, G., Chen, X., Ciais, P.,
645 Grosse, G., Harden, J. W., Hayes, D. J., Hugelius, G., Jafarov, E. E., Krinner, G., Kuhry, P., Lawrence, D.
646 M., Macdougall, A. H., Marchenko, S. S., Mcguire, A. D., Natali, S. M., Nicolsky, D. J., Olefeldt, D.,
647 Peng, S., Romanovsky, V. E., Schaefer, K. M., Strauss, J., Treat, C. C. & Turetsky, M. 2015. A simplified,
648 data-constrained approach to estimate the permafrost carbon-climate feedback. *Philosophical*
649 *Transactions of the Royal Society A: Mathematical, Physical and Engineering Sciences*, 373.

650 L. Kulmala, J. P., P. Hari and T. Vesala: Photosynthesis of ground vegetation in different aged pine forests:
651 Effect of environmental factors predicted with a process-based model, *Journal of Vegetation Science*, 22,
652 96–110, 2011.

653 Launiainen, S., Katul, G. G., Lauren, A., and Kolari, P.: Coupling boreal forest CO₂, H₂O and energy
654 flows by a vertically structured forest canopy – Soil model with separate bryophyte layer, *Ecological*
655 *Modelling*, 312, 385-405, 10.1016/j.ecolmodel.2015.06.007, 2015.

656 Lindo, Z., and Gonzalez, A.: The Bryosphere: An Integral and Influential Component of the Earth's
657 Biosphere, *Ecosystems*, 13, 612-627, 10.1007/s10021-010-9336-3, 2010.

658 Lang, S.I., Cornelissen, J.H.C., Shaver, G.R., Ahrens, M., Callaghan, T.V., Molau, U., Ter Braak, C.J.F.,
659 Hölzer, A. and Aerts, R. (2012), Arctic warming on two continents has consistent negative effects on
660 lichen diversity and mixed effects on bryophyte diversity. *Glob Change Biol*, 18: 1096-1107.
661 <https://doi.org/10.1111/j.1365-2486.2011.02570.x>

662 Longton, R. E.: Adaptations and strategies of polar bryophytes, *Botanical Journal of the Linnean Society*,
663 98, 253-268, 1988.

664 Markham, J. H.: Variation in moss-associated nitrogen fixation in boreal forest stands, *Oecologia*, 161,
665 353-359, 10.1007/s00442-009-1391-0, 2009.

666 McEwing, K. R., Fisher, J. P., and Zona, D.: Environmental and vegetation controls on the spatial
667 variability of CH₄ emission from wet-sedge and tussock tundra ecosystems in the Arctic, *Plant and soil*,
668 388, 37-52, 10.1007/s11104-014-2377-1, 2015.

669 McGuire, A. D., Melillo, J. M., Joyce, L. A., Kicklighter, D. W., Grace, A. L., III, B. M., and Vorosmarty,
670 C. J.: Interactions between carbon and nitrogen dynamics in estimating net primary productivity for
671 potential vegetation in North America, *Global Biogeochemical Cycles*, 6, 101-124, 1992.

672 McGuire, A. D., Melillo, J. M., Kicklighter, D. W., and Joyce, L. A.: Equilibrium responses of soil carbon
673 to climate change: Empirical and process-based estimates, *Journal of Biogeography*, 785-796, 1995.

674 McGuire, A. D., and Hobbie, J. E.: Global climate change and the equilibrium responses of carbon
675 storage in arctic and subarctic regions, In *Modeling the Arctic system: A workshop report on the state of*
676 *modeling in the Arctic System Science program*, 53-54, 1997.

677 McGuire, A. D., Anderson, L. G., Christensen, T. R., Dallimore, S., Guo, L., Hayes, D. J., Heimann, M.,
678 Lorenson, T. D., Macdonald, R. W., and Roulet, N.: Sensitivity of the carbon cycle in the Arctic to climate
679 change, *Ecological Monographs*, 79, 523-555, 2009.

680 Melillo, J. M., McGuire, A. D., Kicklighter, D. W., Moore, B., Vorosmarty, C. J., and Schloss, A. L.:
681 Global climate change and terrestrial net primary production, *Nature*, 363, 234, 10.1038/363234a0, 1993.

682 Melillo, J. M., Butler, S., Johnson, J., Mohan, J., Steudler, P., Lux, H., Burrows, E., Bowles, F., Smith, R.,
683 Scott, L., Vario, C., Hill, T., Burton, A., Zhou, Y.-M., and Tang, J.: Soil warming, carbon - nitrogen
684 interactions, and forest carbon budgets, *PNAS*, 108, 9508-9512, 2011.

685 Naomi Oreskes, K. S.-F., Kenneth Belitz: Verification, validation, and confirmation of numerical models
686 in the earth sciences, *Science*, 263, 641-646, 1994.

687 O. Skre, W. C. O.: Moss production in a black spruce *Picea mariana* forest with permafrost near
688 Fairbanks, Alaska, as compared with two permafrost-free stands, *Ecography*, 2, 249-254, 1979.

689 Oechel, W. C., Laskowski, C. A., Burba, G., Gioli, B., and Kalhori, A. A. M.: Annual patterns and budget
690 of CO₂ flux in an Arctic tussock tundra ecosystem, *Journal of Geophysical Research: Biogeosciences*,
691 119, 323-339, 10.1002/2013jg002431, 2014.

692 Okland, R. H.: Population Biology of the Clonal Moss *Hylocomium Splendens* in Norwegian Boreal
693 Spruce Forests. I. Demography, *Journal of Ecology*, 83, 697-712, 1995.

694 P.C. Harley, J. D. T., K.J. Murray, and J. Beyers: Irradiance and temperature effects on photosynthesis of
695 tussock tundra *Sphagnum* mosses from the foothills of the Philip Smith Mountains, Alaska, *Oecologia*,
696 79, 251-259, 1989.

697 Pakarinen, P., and D. H. Vitt: Primary production of plant communities of the Truelove Lowland, Devon
698 Island, Canada—Moss communities, Primary production and production processes, tundra biome.
699 International Biological Programme, Tundra Biome Steering Committee, Edmonton Oslo, 37-46, 1973.

700 Pharo, E. J., and Zartman, C. E.: Bryophytes in a changing landscape: The hierarchical effects of habitat
701 fragmentation on ecological and evolutionary processes, *Biological Conservation*, 135, 315-325,
702 10.1016/j.biocon.2006.10.016, 2007.

703 Raich, J. W., Rastetter, E. B., Melillo, J. M., Kicklighter, D. W., Steudler, P. A., Peterson, B. J., Grace, A.
704 L., III, B. M., and Vorosmarty, C. J.: Potential net primary productivity in South America: application of a
705 global model, *Ecological Applications*, 1, 399-429, 1991.

706 Richardson, A. D., Jenkins, J. P., Braswell, B. H., Hollinger, D. Y., Ollinger, S. V., and Smith, M. L.: Use
707 of digital webcam images to track spring green-up in a deciduous broadleaf forest, *Oecologia*, 152, 323-
708 334, 10.1007/s00442-006-0657-z, 2007.

709 Running, S. W., and Coughlan, J. C.: A general model of forest ecosystem processes for regional
710 applications I. Hydrologic balance, canopy gas exchange and primary production processes., *Ecological*
711 *Modelling*, 42, 125-154, 1988.

712 S. Frohking, M. L. G., S.C. Wofsy, S-M. Fan, D.J. Sutton, J.W. Munger, A.M. Bazzaz, B.C. Daube, P.M.
713 Crill, J.D, Aber, L.E. Band, X. Wang, K. Savage, T. Moore and R.C. Harriss: Modelling temporal
714 variability in the carbon balance of a spruce/moss boreal forest, *Global change biology*, 2, 343-366, 1996.

715 Sarah E. Hobbie, J. P. S., Susan E. Trumbore and James R. Randerson: Controls over carbon storage and
716 turnover in high-latitude soils, *Global change biology*, 6, 196-210, 2000.

717 Schimel, D. S., House, J. I., Hibbard, K. A., Bousquet, P., Ciais, P., Peylin, P., Braswell, B. H., Apps, M.
718 J., Baker, D., Bondeau, A., Canadell, J., Churkina, G., Cramer, W., Denning, A. S., Field, C. B.,
719 Friedlingstein, P., Goodale, C., Heimann, M., Houghton, R. A., Melillo, J. M., III, B. M., Murdiyarso, D.,
720 Noble, I., Pacala, S. W., Prentice, I. C., Raupach, M. R., Rayner, P. J., Scholes, R. J., Steffen, W. L., and

721 Wirth, C.: Recent patterns and mechanisms of carbon exchange by terrestrial ecosystems, *Nature*, 414,
722 2001.

723 Serreze, M. C., and Francis, J. A.: The Arctic on the fast track of change, *Weather*, 61, 65-69, 2006.

724 Shetler, G., Turetsky, M. R., Kane, E., and Kasischke, E.: Sphagnum mosses limit total carbon
725 consumption during fire in Alaskan black spruce forests, *Canadian Journal of Forest Research*, 38, 2328-
726 2336, 10.1139/x08-057, 2008.

727 Soja, A. J., Tchepakova, N. M., French, N. H. F., Flannigan, M. D., Shugart, H. H., Stocks, B. J.,
728 Sukhinin, A. I., Parfenova, E. I., Chapin, F. S., and Stackhouse, P. W.: Climate-induced boreal forest
729 change: Predictions versus current observations, *Global and Planetary Change*, 56, 274-296,
730 10.1016/j.gloplacha.2006.07.028, 2007.

731 Stow, D. A., Hope, A., McGuire, D., Verbyla, D., Gamon, J., Huemmrich, F., Houston, S., Racine, C.,
732 Sturm, M., Tape, K., Hinzman, L., Yoshikawa, K., Tweedie, C., Noyle, B., Silapaswan, C., Douglas, D.,
733 Griffith, B., Jia, G., Epstein, H., Walker, D., Daeschner, S., Petersen, A., Zhou, L., and Myneni, R.:
734 Remote sensing of vegetation and land-cover change in Arctic Tundra Ecosystems, *Remote Sensing of*
735 *Environment*, 89, 281-308, 10.1016/j.rse.2003.10.018, 2004.

736 T. G. Williams, L. B. F.: Measuring and modelling environmental influences on photosynthetic gas
737 exchange in Sphagnum and Pleurozium, *Plant, Cell and Environment*, 21, 555-564, 1998.

738 Tang, J., and Zhuang, Q.: Equifinality in parameterization of process-based biogeochemistry models: A
739 significant uncertainty source to the estimation of regional carbon dynamics, *Journal of Geophysical*
740 *Research: Biogeosciences*, 113, 10.1029/2008jg000757, 2008.

741 Tape, K. E. N., Sturm, M., and Racine, C.: The evidence for shrub expansion in Northern Alaska and the
742 Pan-Arctic, *Global change biology*, 12, 686-702, 10.1111/j.1365-2486.2006.01128.x, 2006.

743 Tarnocai, C., Canadell, J. G., Schuur, E. A. G., Kuhry, P., Mazhitova, G., and Zimov, S.: Soil organic
744 carbon pools in the northern circumpolar permafrost region, *Global Biogeochemical Cycles*, 23, n/a-n/a,
745 10.1029/2008gb003327, 2009.

746 Todd-Brown, K. E. O., Randerson, J. T., Post, W. M., Hoffman, F. M., Tarnocai, C., Schuur, E. A. G., and
747 Allison, S. D.: Causes of variation in soil carbon simulations from CMIP5 Earth system models and
748 comparison with observations, *Biogeosciences*, 10, 1717-1736, 10.5194/bg-10-1717-2013, 2013.

749 Treseder, K. K., Balser, T. C., Bradford, M. A., Brodie, E. L., Dubinsky, E. A., Eviner, V. T., Hofmockel,
750 K. S., Lennon, J. T., Levine, U. Y., MacGregor, B. J., Pett-Ridge, J., and Waldrop, M. P.: Integrating
751 microbial ecology into ecosystem models: challenges and priorities, *Biogeochemistry*, 109, 7-18,
752 10.1007/s10533-011-9636-5, 2011.

753 Treseder, K. K., Marusenko, Y., Romero-Olivares, A. L., and Maltz, M. R.: Experimental warming alters
754 potential function of the fungal community in boreal forest, *Global change biology*, 22, 3395-3404,
755 10.1111/gcb.13238, 2016.

756 Turetsky, M. R., Mack, M. C., Hollingsworth, T. N., and Harden, J. W.: The role of mosses in ecosystem
757 succession and function in Alaska's boreal forest ~~This article is one of a selection of papers from The~~
758 ~~Dynamics of Change in Alaska's Boreal Forests: Resilience and Vulnerability in Response to Climate~~
759 ~~Warming~~, *Canadian Journal of Forest Research*, 40, 1237-1264, 10.1139/x10-072, 2010.

760 Turetsky, M. R., Bond-Lamberty, B., Euskirchen, E., Talbot, J., Frohling, S., McGuire, A. D., and Tuittila,
761 E. S.: The resilience and functional role of moss in boreal and arctic ecosystems, *The New phytologist*,
762 196, 49-67, 10.1111/j.1469-8137.2012.04254.x, 2012.

763 Wardle, M.-C. N. a. D. A.: Understory vegetation as a forest ecosystem driver: evidence from the northern
764 Swedish boreal forest, *The Ecological Society of America*, 3, 421–428, 2005.

765 White, A., Cannell, M. G. R., and Friend, A. D.: The high-latitude terrestrial carbon sink: a model analysis
766 *Global change biology*, 6, 227-245, 2000.

767 Wieder, W. R., Bonan, G. B., and Allison, S. D.: Global soil carbon projections are improved by
768 modelling microbial processes, *Nature Climate Change*, 3, 909-912, 10.1038/nclimate1951, 2013.

769 Zha, J., and Zhuang, Q.: Microbial decomposition processes and vulnerable Arctic soil organic carbon in
770 the 21st century, *Biogeosciences Discussions*, 1-34, 10.5194/bg-2018-241, 2018.

771 Zhuang, Q., Romanovsky, V. E., and McGuire, A. D.: Incorporation of a permafrost model into a large-
772 scale ecosystem model: Evaluation of temporal and spatial scaling issues in simulating soil thermal
773 dynamics, *Journal of Geophysical Research: Atmospheres*, 106, 33649-33670, 10.1029/2001jd900151,
774 2001.

775 Zhuang, Q., McGuire, A. D., O'Neill, K. P., Harden, J. W., Romanovsky, V. E., and Yarie, J.: Modeling
776 soil thermal and carbon dynamics of a fire chronosequence in interior Alaska, *Journal of Geophysical*
777 *Research*, 108, 10.1029/2001jd001244, 2002.

778 Zhuang, Q., A. D. McGuire, J. M. Melillo, J. S. Clein, R. J. Dargaville, D. W. Kicklighter, R. B. Myneni,
779 J. Dong, V. E. Romanovsky, J. Harden, J. E. Hobbie (2003) Carbon cycling in extratropical terrestrial
780 ecosystems of the Northern Hemisphere during the 20th Century: A modeling analysis of the influences of
781 soil thermal dynamics, *Tellus*, 55B, 751-776, 2003

782 Zhuang, Q., He, J., Lu, Y., Ji, L., Xiao, J., and Luo, T.: Carbon dynamics of terrestrial ecosystems on the
783 Tibetan Plateau during the 20th century: an analysis with a process-based biogeochemical model, *Global*
784 *Ecology and Biogeography*, 19, 649-662, 10.1111/j.1466-8238.2010.00559.x, 2010.

785 Zhuang, Q., Chen, M., Xu, K., Tang, J., Saikawa, E., Lu, Y., Melillo, J. M., Prinn, R. G., and McGuire, A.
786 D.: Response of global soil consumption of atmospheric methane to changes in atmospheric climate and
787 nitrogen deposition, *Global Biogeochemical Cycles*, 27, 650-663, 10.1002/gbc.20057, 2013.

788 Zhuang, Q., Zhu, X., He, Y., Prigent, C., Melillo, J. M., David McGuire, A., Prinn, R. G., and Kicklighter,
789 D. W.: Influence of changes in wetland inundation extent on net fluxes of carbon dioxide and methane in
790 northern high latitudes from 1993 to 2004, *Environmental Research Letters*, 10, 095009, 10.1088/1748-
791 9326/10/9/095009, 2015.

792

793

794

795

796

797

798

799 **Author contributions.** Q.Z. designed the study. J.Z. conducted model development, simulation
800 and analysis. J.Z. and Q. Z. wrote the paper.

801 **Competing financial interests.** The submission has no competing financial interests.

802 **Materials & Correspondence.** Correspondence and material requests should be addressed to
803 qzhuang@purdue.edu.

804

805

806

807

808

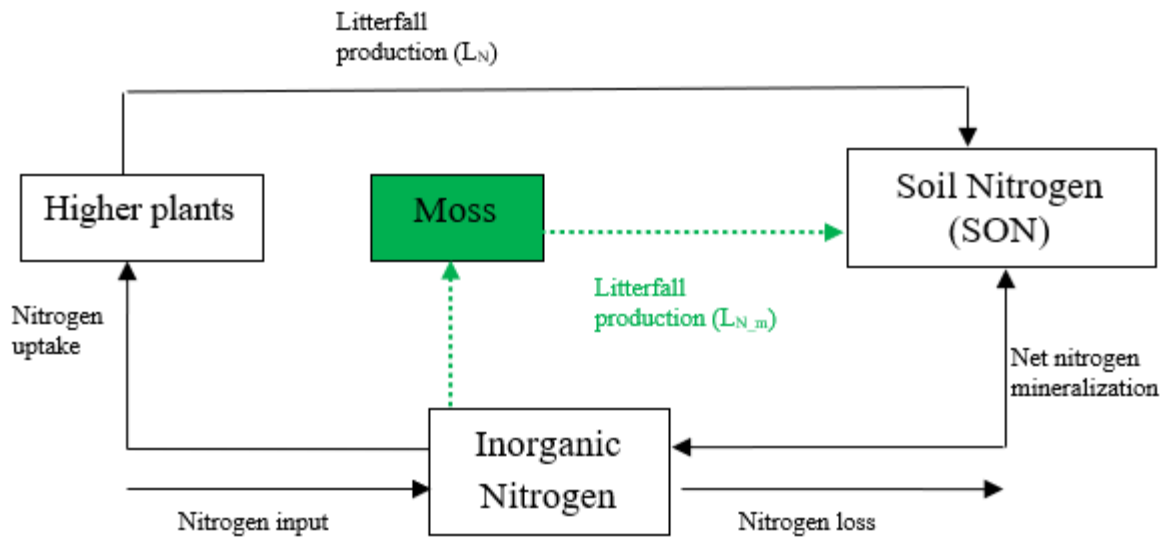
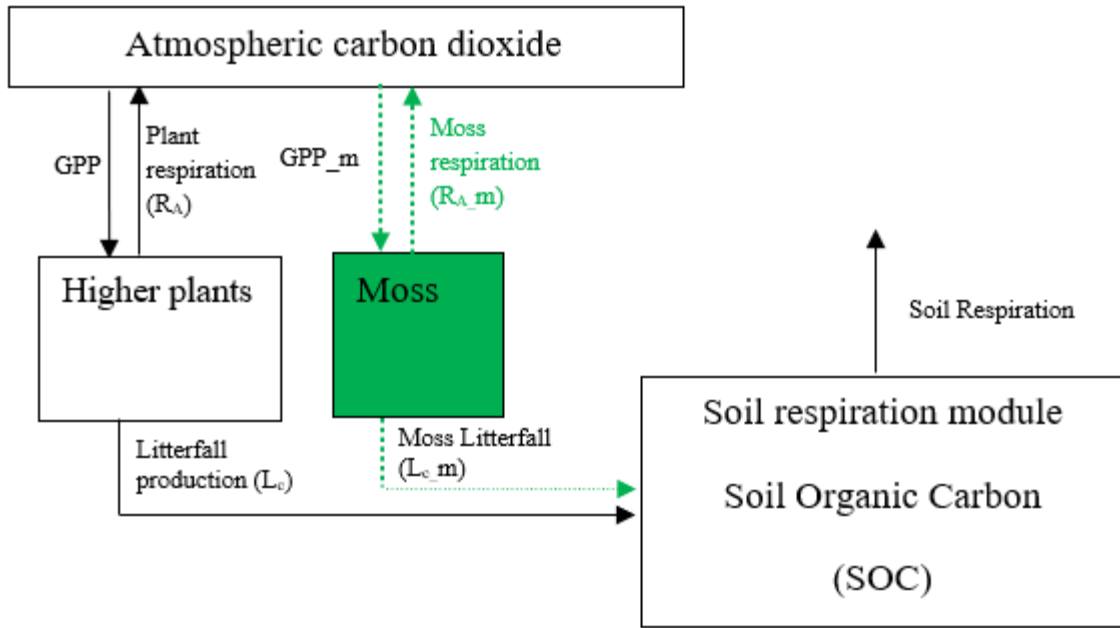
809

810

811

812

813

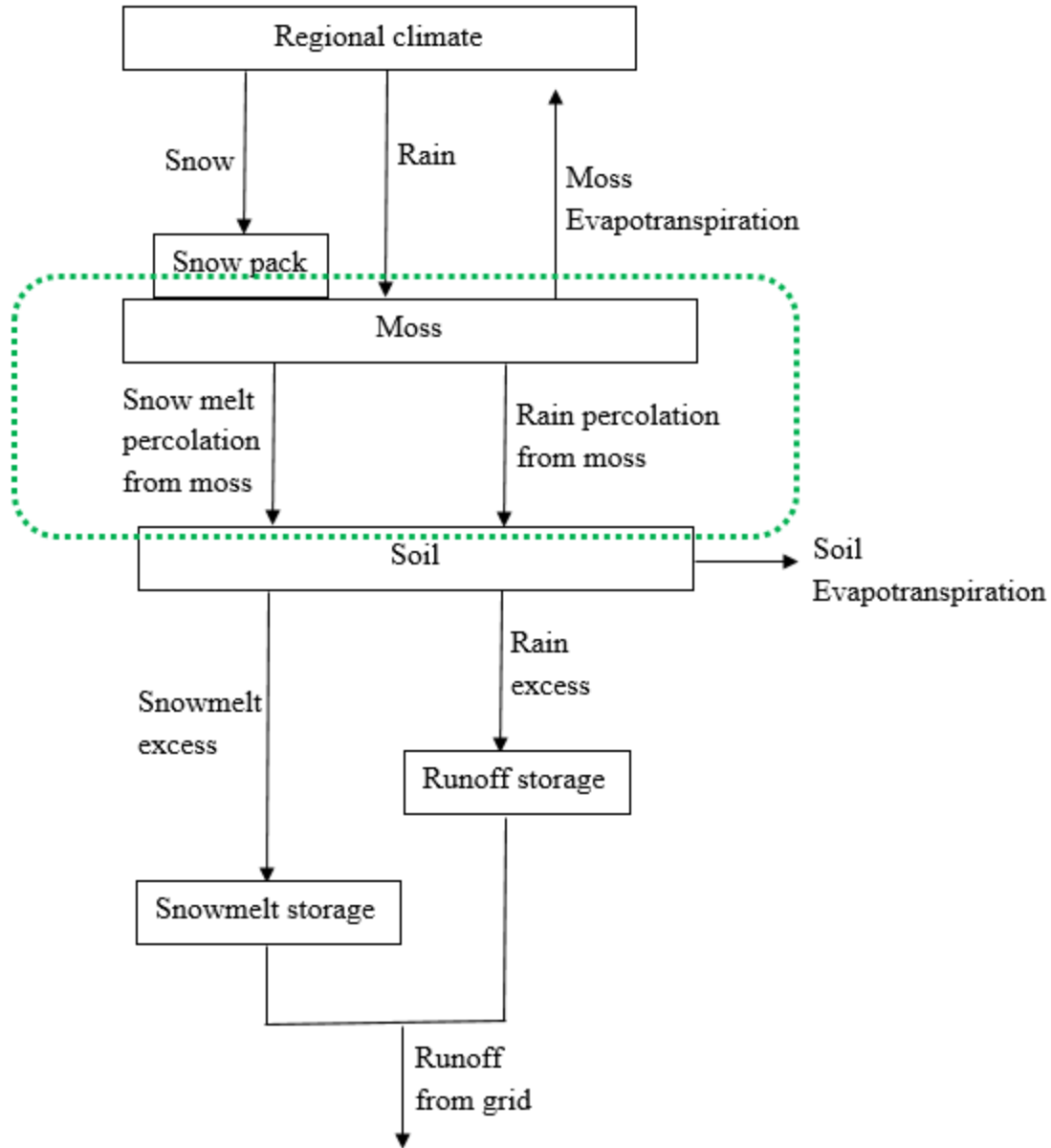


814

815 Figure 1. Schematic diagram of TEM_Moss: Green dashed arrows are new carbon and nitrogen
 816 fluxes, representing moss production, moss respiration and litterfall of moss. Black arrows were
 817 in TEM 5.0 (Zhuang et al., 2013).

818

819



820

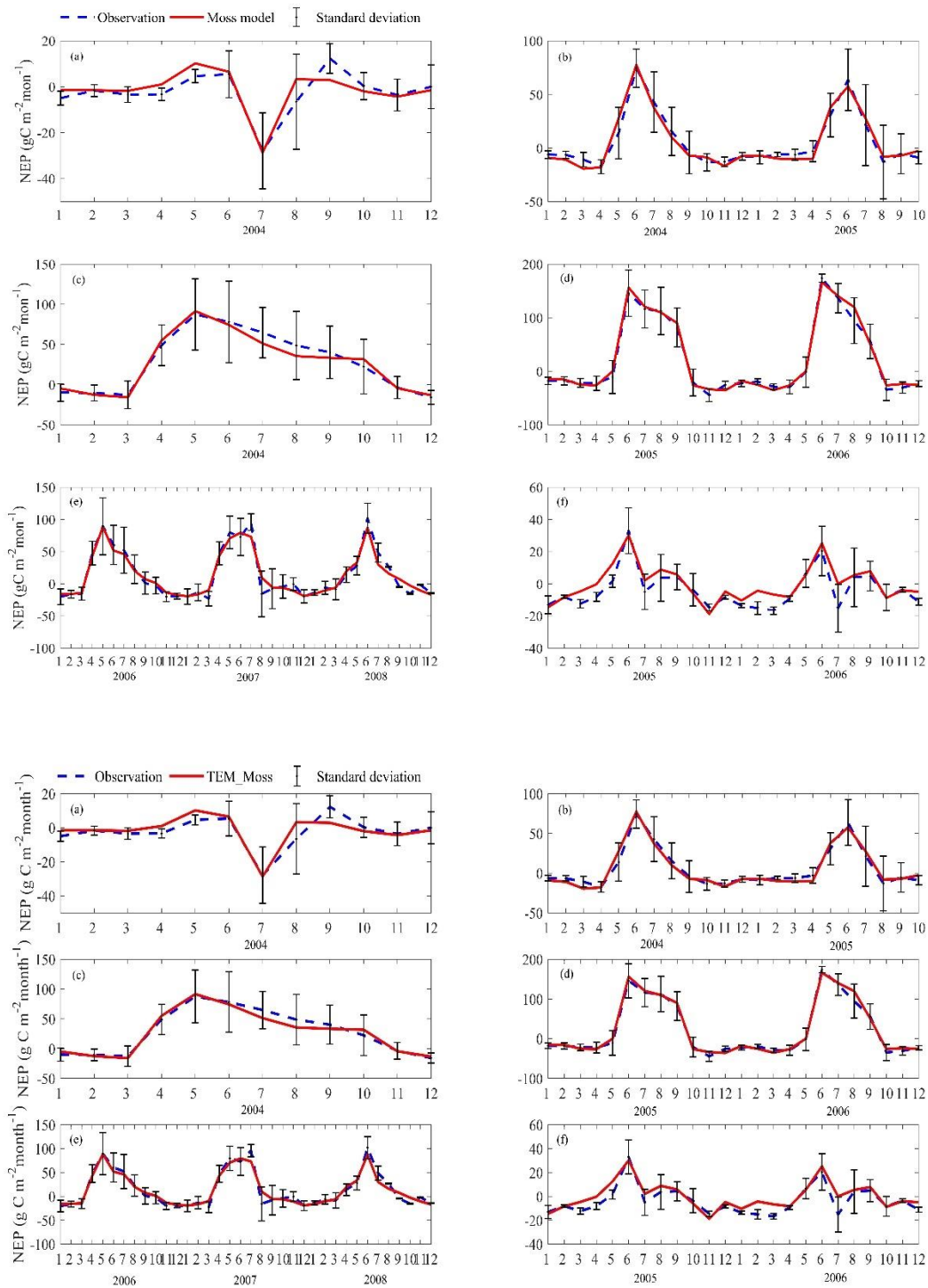
821 Figure 2. The revised Water Balance Model: Green dashed circle represents the hydrology
 822 dynamics for moss (Vörösmarty et al., 1989).

823

824

825

826

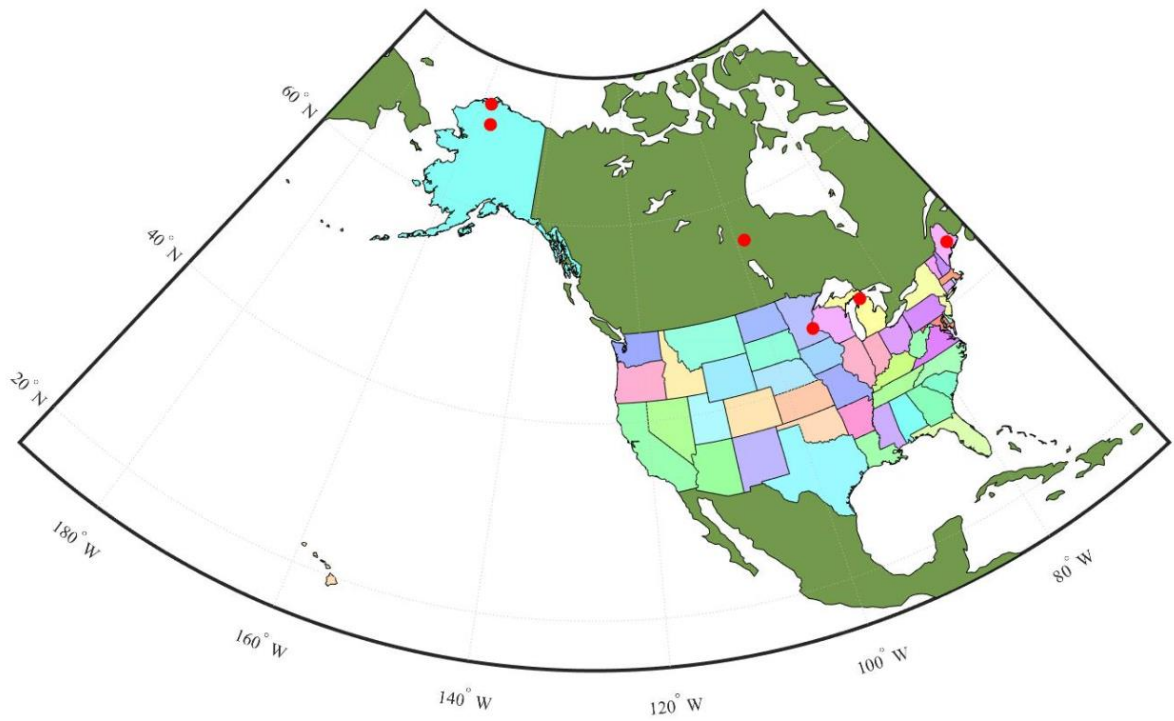


827

828

829 Figure 3. Comparison between observed and simulated NEP ($\text{g C m}^{-2}\text{month}^{-1}$) at: (a) Ivotuk
 830 (alpine tundra), (b) UCI-1964 burn site (boreal forest), (c) Howland Forest-(~~main tower~~)
 831 (temperate coniferous forest), (d) Univ. of Mich. Biological Station (Temperate deciduous
 832 forest), (e) KUOM Turfgrass Field (Grassland), and (f) Atqasuk (Wet tundra). ~~Note: scales are~~
 833 ~~different.~~ Error bars represent standard errors among daily ~~measure data~~.

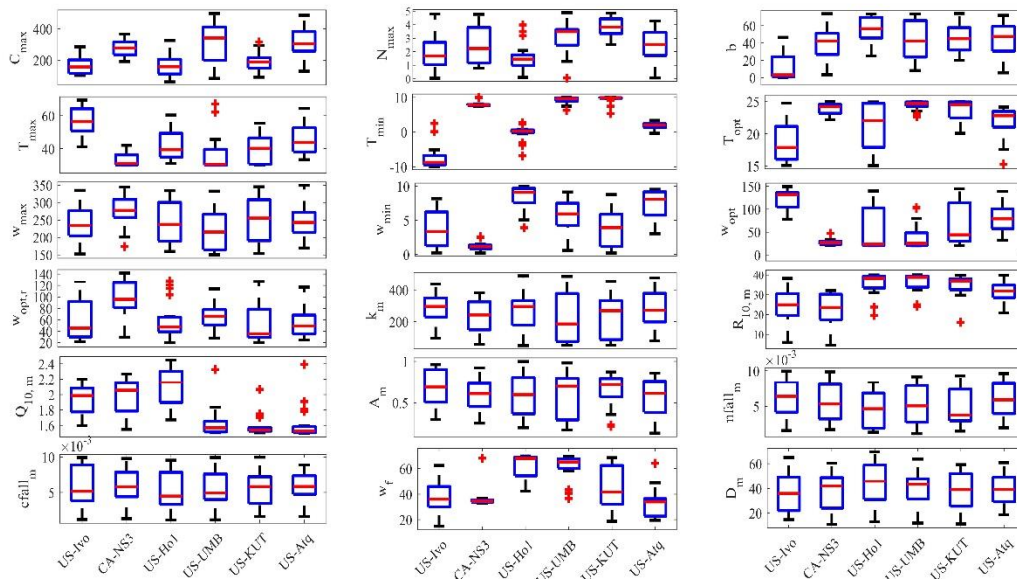
834
835
836
837
838
839
840
841
842



843
844
845
846
847
848
849
850
851
852

Figure 4. Map showing six sites used for TEM_Moss calibration. The red points represent the six sites, five are in the US and one is in the Canada: US-Ivo: Ivotuk (alpine tundra), CA-NS3: UCI-1964 burn site (boreal forest), US-Ho1: Howland Forest (temperate coniferous forest), US-UMB: Univ. of Mich. Biological Station (temperate deciduous forest), US-KUT: KUOM Turfgrass Field (grassland), US-Atq: Atqasuk (wet tundra).

853
 854
 855
 856
 857
 858
 859
 860

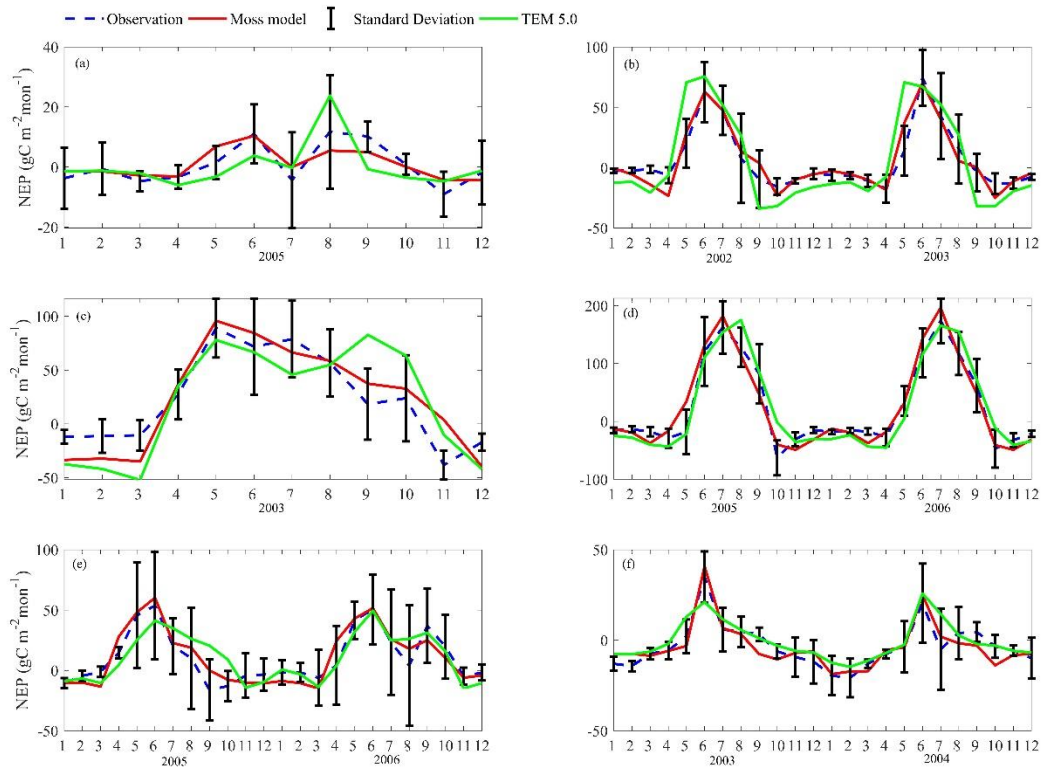


861

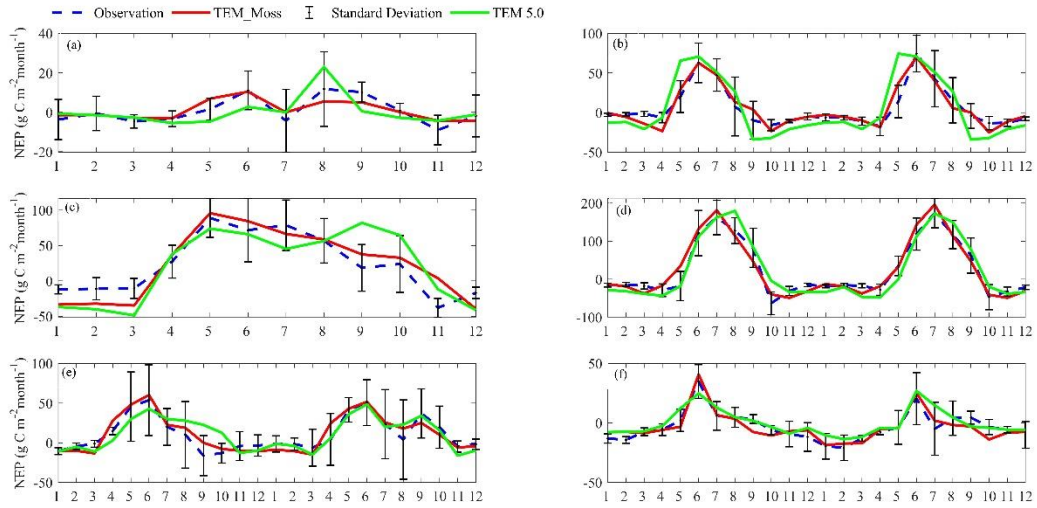
862 Figure 5. Boxplot of parameter posterior distribution that are obtained after ensemble inverse
 863 modeling for TEM_Moss at all six sites: US-Ivo: Ivotuk (alpine tundra), CA-NS3: UCI-1964
 864 burn site (boreal forest), US-Ho1: Howland Forest (temperate coniferous forest), US-UMB:
 865 Univ. of Mich. Biological Station (temperate deciduous forest), US-KUT: KUOM Turfgrass
 866 Field (grassland), US-Atq: Atqasuk (wet tundra). Boxes represent the range between the first
 867 quartile and the third quartile of the parameter values, the red line within box represents the
 868 second quartile or the mean of the values. The bottom and top whiskers represent minimum and
 869 maximum parameter values, respectively.

870
 871
 872
 873

874
875
876
877
878
879



880



881

882

883 Figure 6. Comparison between observed and simulated NEP ($\text{g}_C \text{m}^{-2} \text{month}^{-1}$) at: (a) Ivotuk
 884 (alpine tundra), (b) UCI-1964 burn site (boreal forest), (c) Howland Forest (main tower)
 885 (temperate coniferous forest), (d) Bartlett Experimental Forest (Temperate deciduous forest), (e)
 886 Brookings (Grassland), and (f) Atqasuk (Wet tundra). ~~Note: scales are different.~~

887

888

889

890

891

892

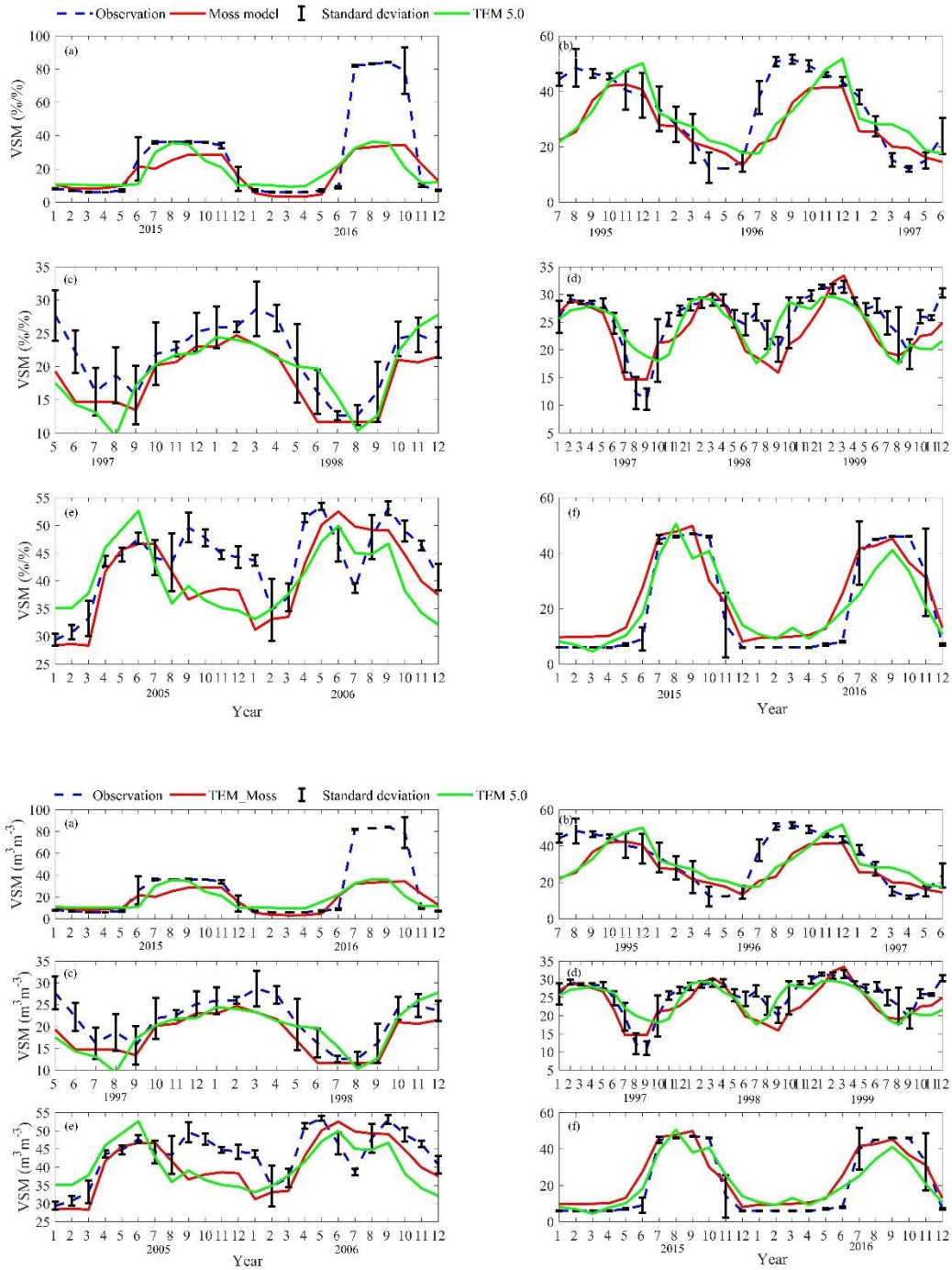
893

894

895

896

897



898

899

900 Figure 7. Comparison between observed and simulated volumetric soil moisture (VSM, m^3m^{-3})
 901 $\%/%$) at: (a) US-Ivo (alpine tundra), (b) BOREAS NSA-OBS (boreal forest), (c) NL-Loo
 902 (temperate coniferous forest), (d) DK-Sor (Temperate deciduous forest), (e) US-Bkg
 903 (Grassland), and (f) US-Atq (Wet tundra). Note: scales are different.

904

905

906

907

908

909

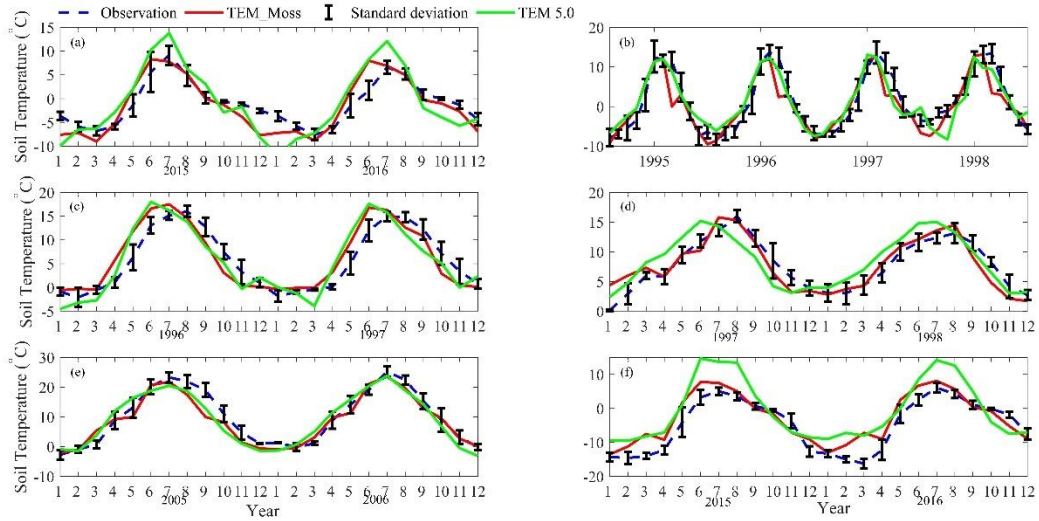
910

911

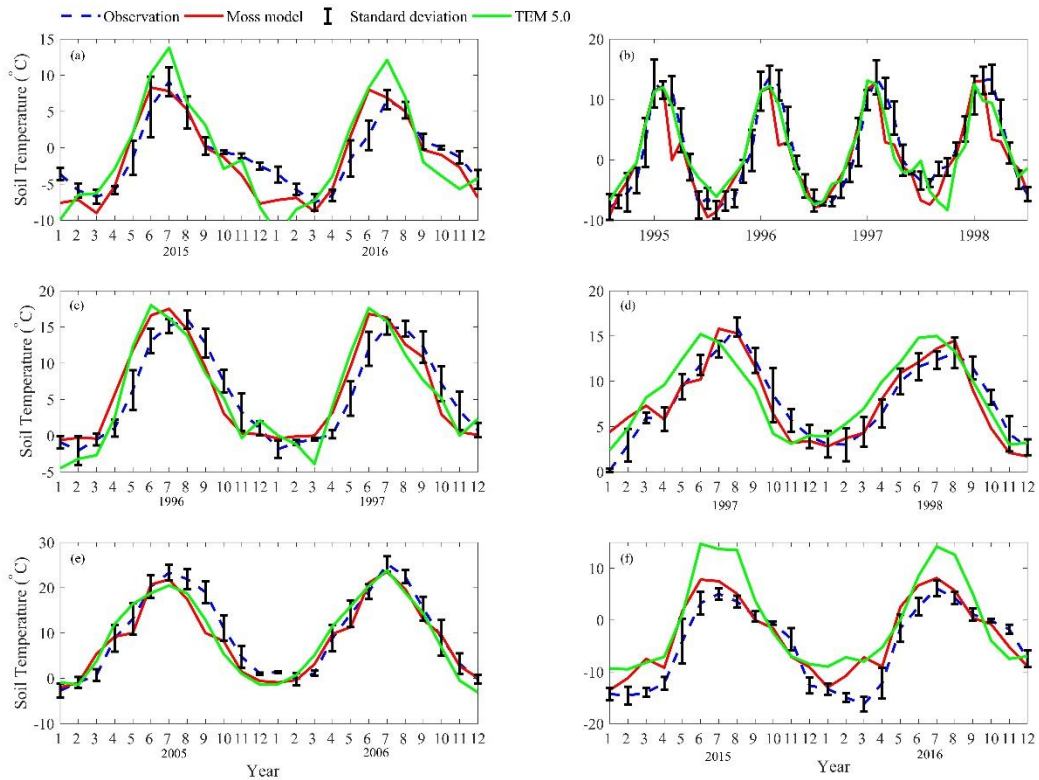
912

913

914



915



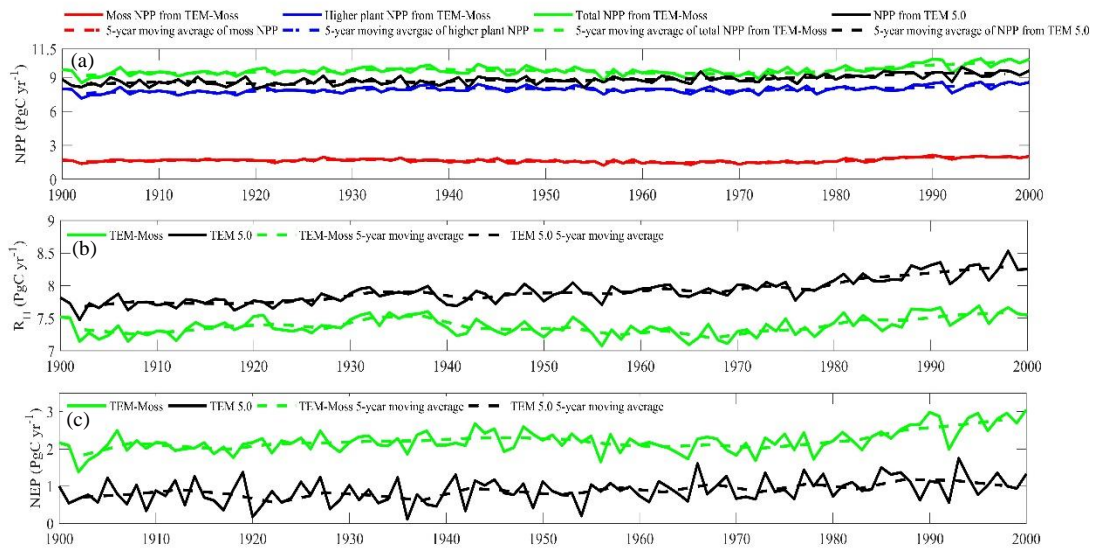
916

917 Figure 8. Comparison between observed and simulated soil temperature at 5cm depth (°C) at: (a)
 918 US-Ivo (alpine tundra), (b) BOREAS NSA-OBS (boreal forest), (c) US-Ho1 (temperate
 919 coniferous forest), (d) BE-Vie (Temperate deciduous forest), (e) US-Bkg (Grassland), and (f)
 920 US-Atq (Wet tundra). Note: scales are different.

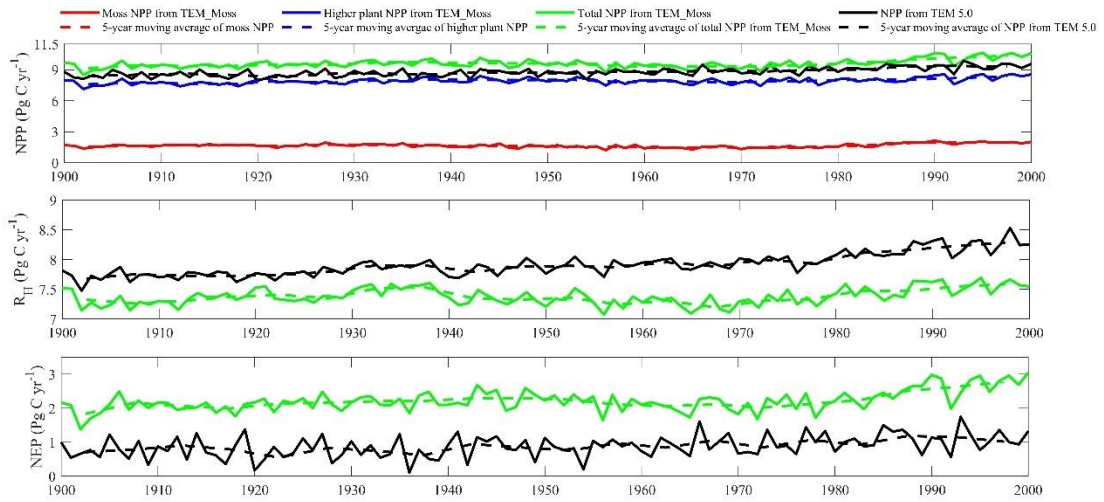
921

922

923
924
925
926
927
928
929
930
931
932



933



934

935 Figure 9. Simulated annual net primary production (NPP, a), heterotrophic respiration (R_H , b),
 936 and net ecosystem production (NEP, c) during the 20th century by TEM_Moss and TEM 5.0.

937

938

939

940

941

942

943

944

945

946

947

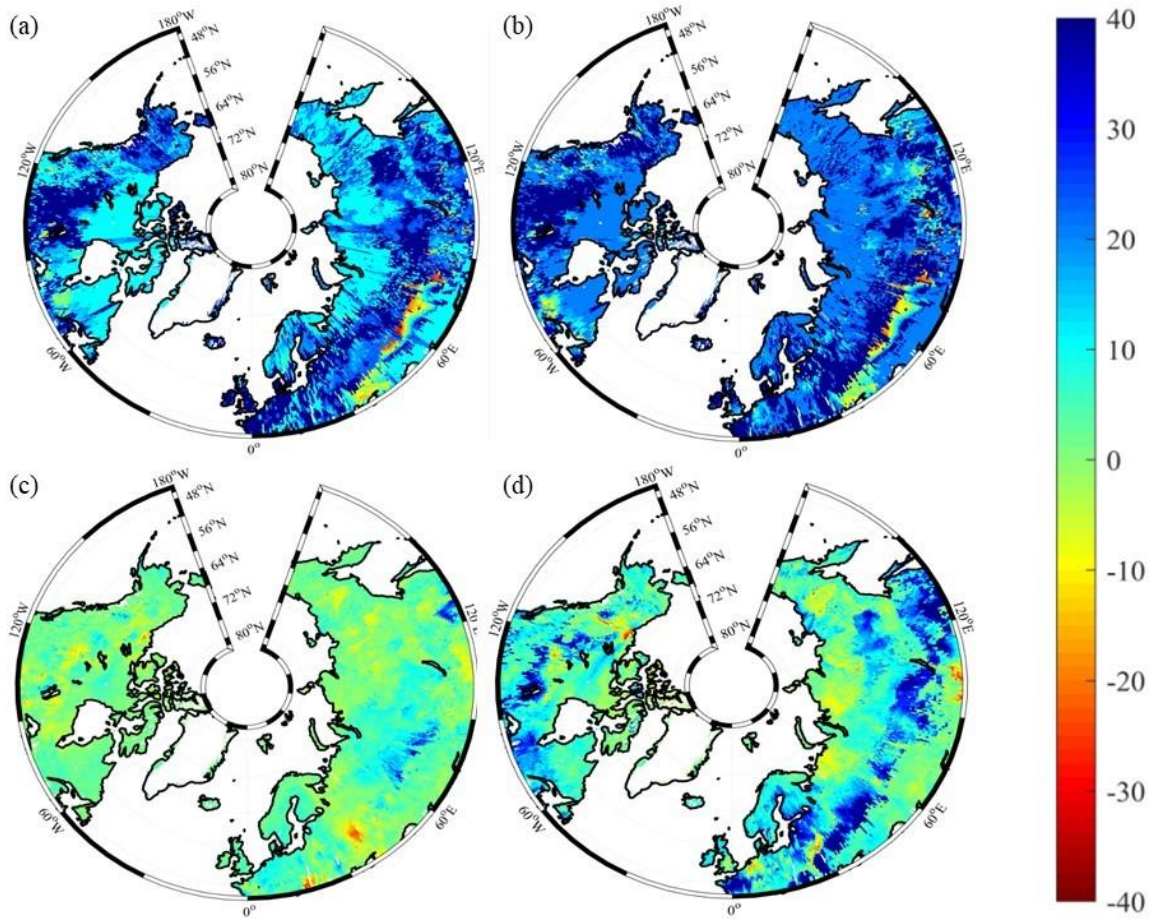
948

949

950

951

952



953

954 Figure 10. Spatial distribution of NEP simulated by TEM_Moss for the periods (a) 1900–1950,
 955 (b) 1951–2000, and by TEM 5.0 for the periods (c) 1900–1950, (d) 1951–2000. Positive values
 956 of NEP represent sinks of CO₂ into terrestrial ecosystems, while negative values represent
 957 sources of CO₂ to the atmosphere.

958

959

960

961

962

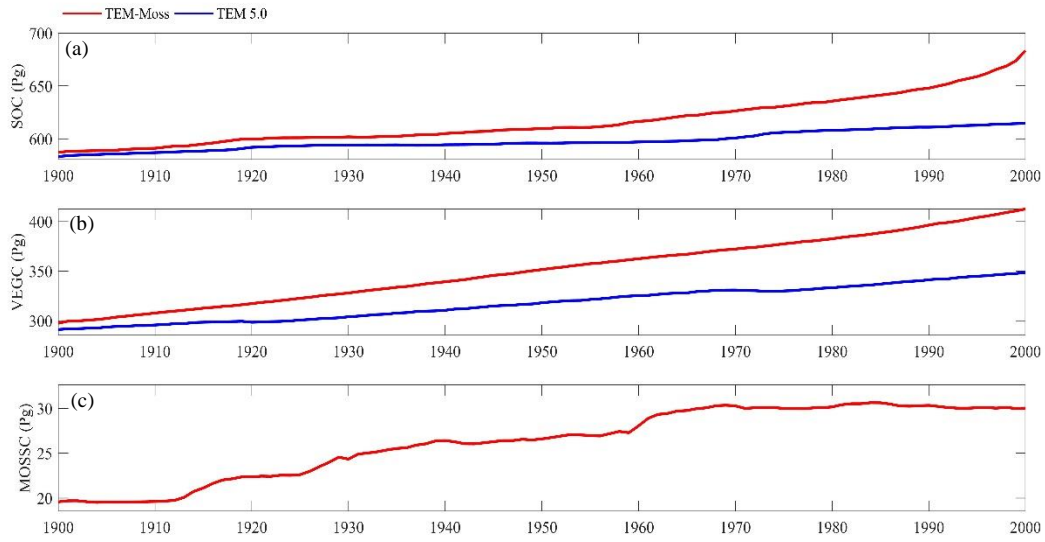
963

964

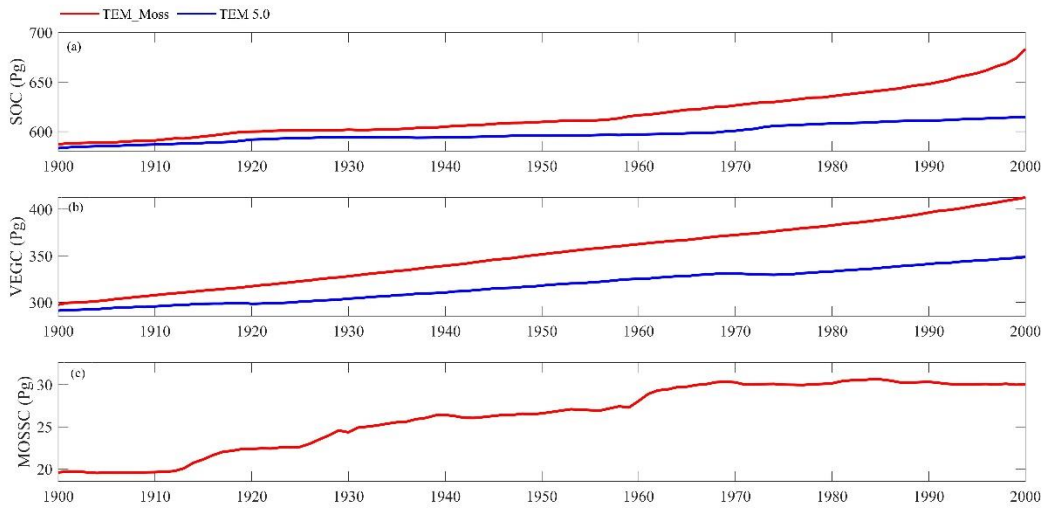
965

966

967



968



969

970 Figure 11. Simulated annual soil organic carbon (SOC, a), vegetation carbon (VEGC, b), and
 971 moss carbon (MOSSC, c) during the 20th century by TEM_Moss and TEM 5.0.

972

973

974

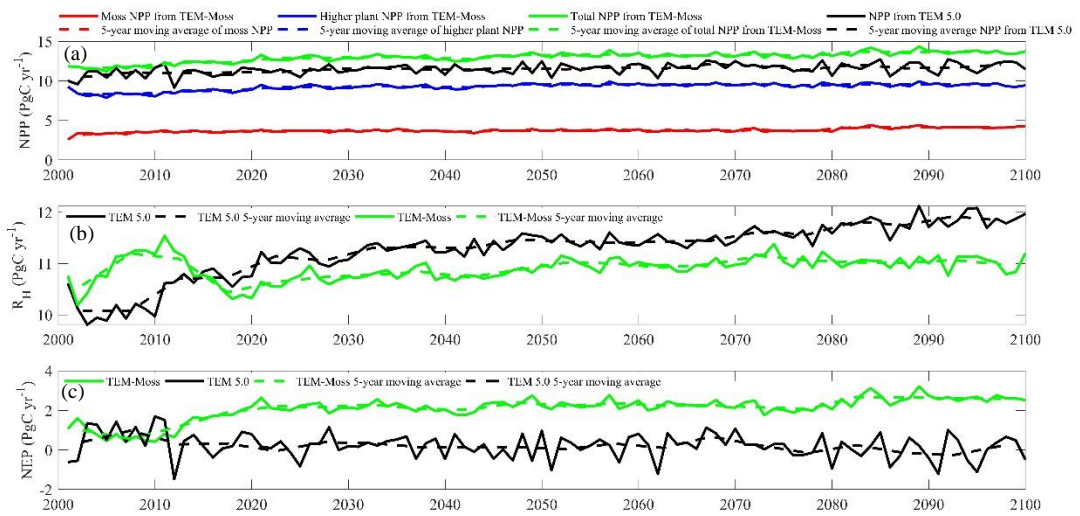
975

976

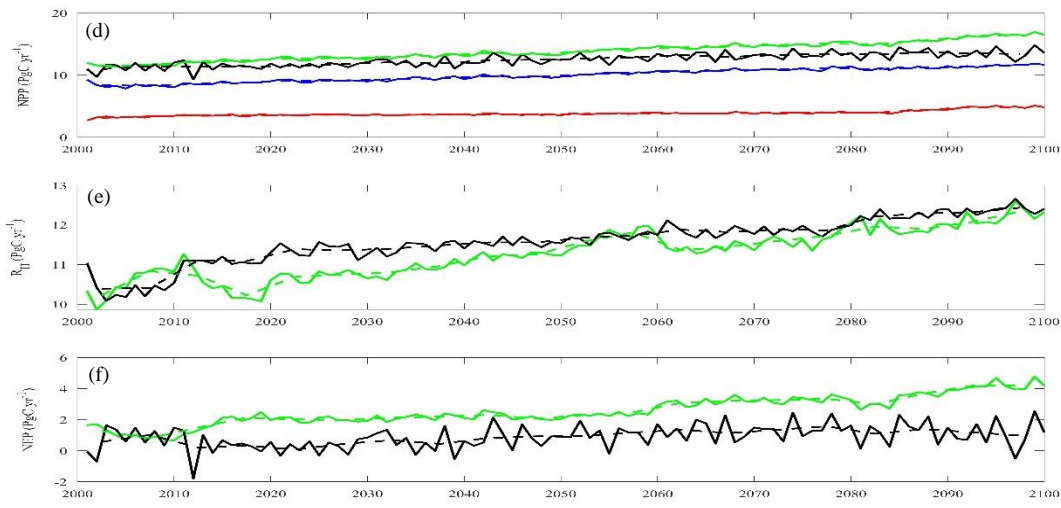
977

978

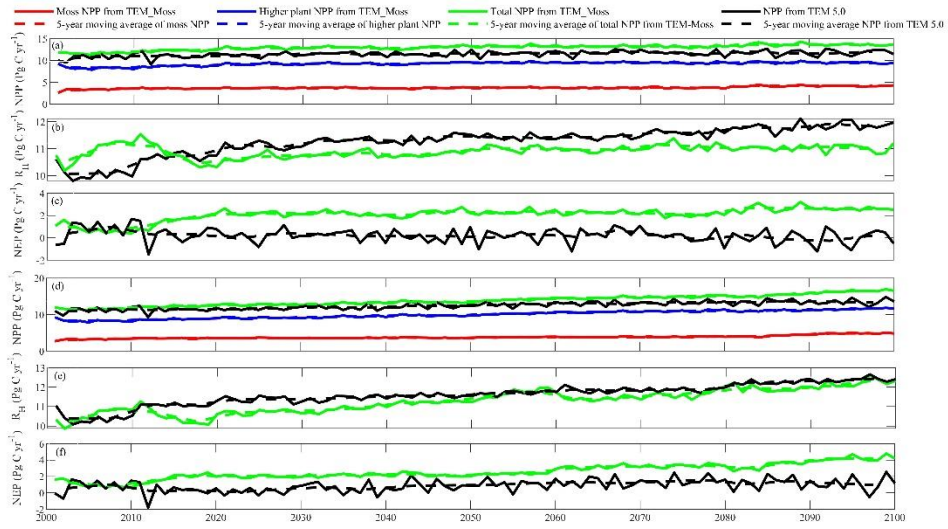
979
980
981
982
983
984
985
986
987
988



989



990



991

992 Figure 12. Predicted changes in carbon fluxes: annual net primary production (NPP, (a, d)),
 993 heterotrophic respiration (R_H , (b, e)), and net ecosystem production (NEP, (c, f)) during the 21st
 994 century under RCP 2.6 scenario (a, b, c, **upper panel**) and RCP 8.5 scenario (d, e, f, **bottom**
 995 **panel**) by TEM_Moss and TEM 5.0.

996

997

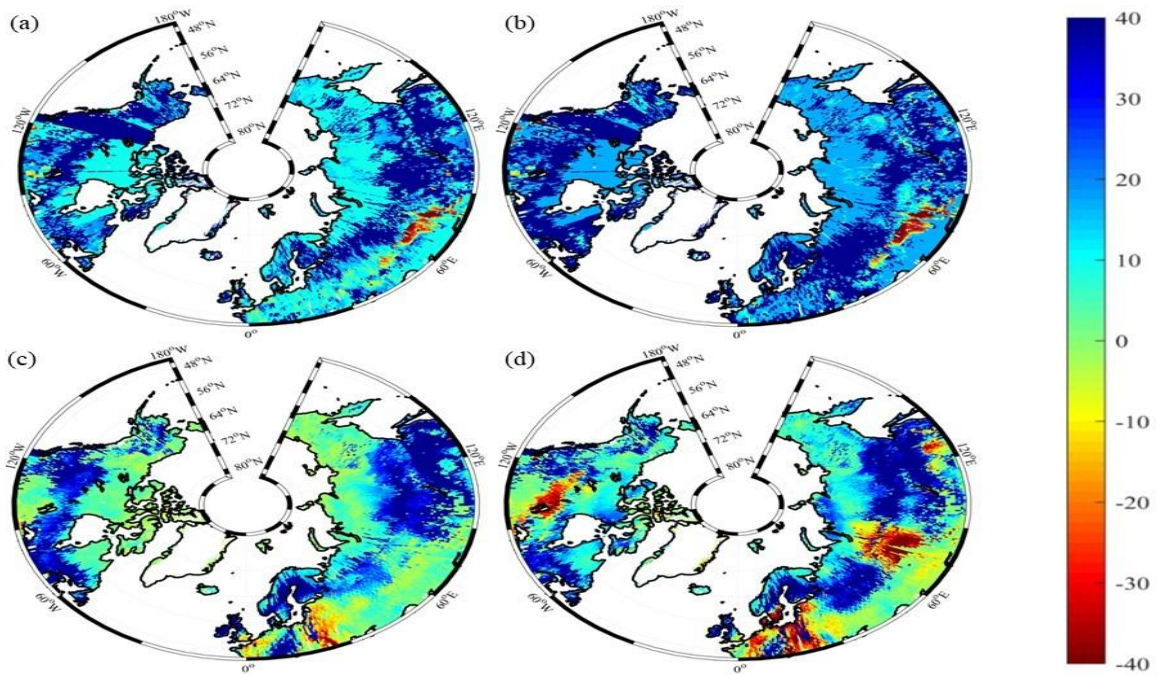
998

999

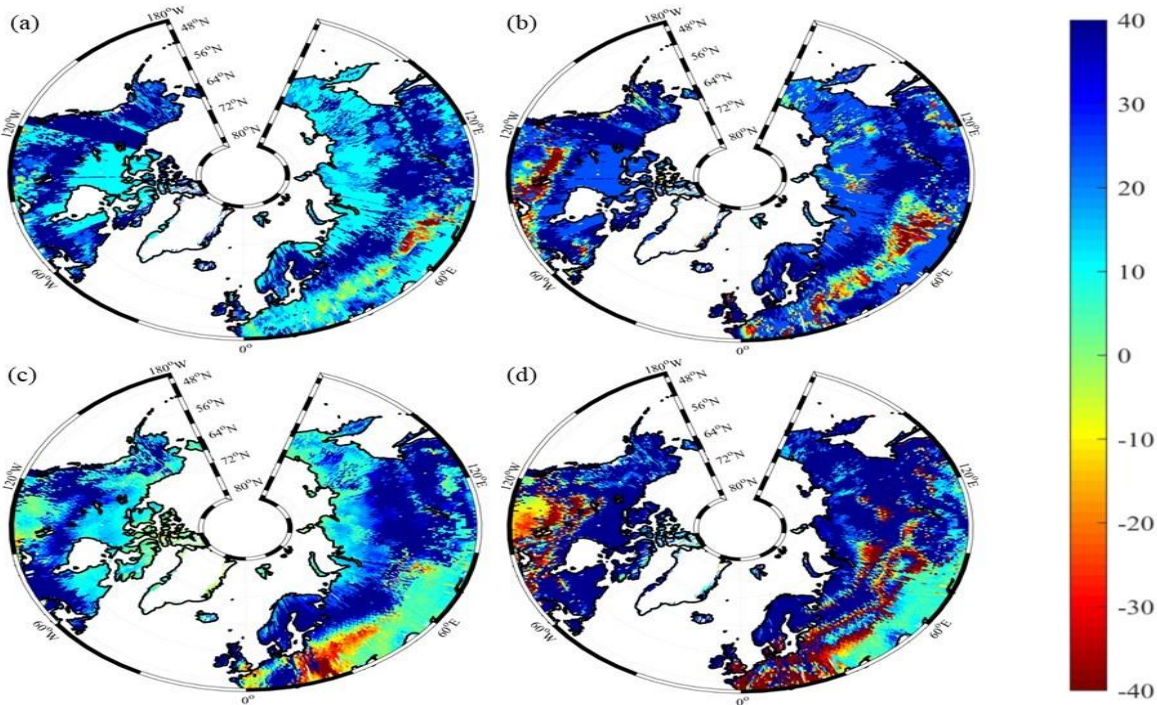
1000

1001

1002



1003

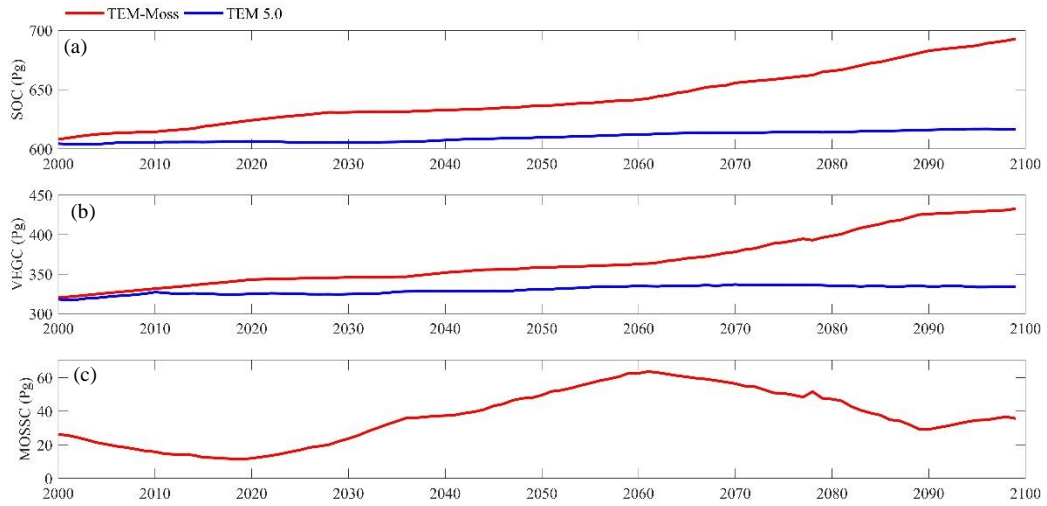


1004

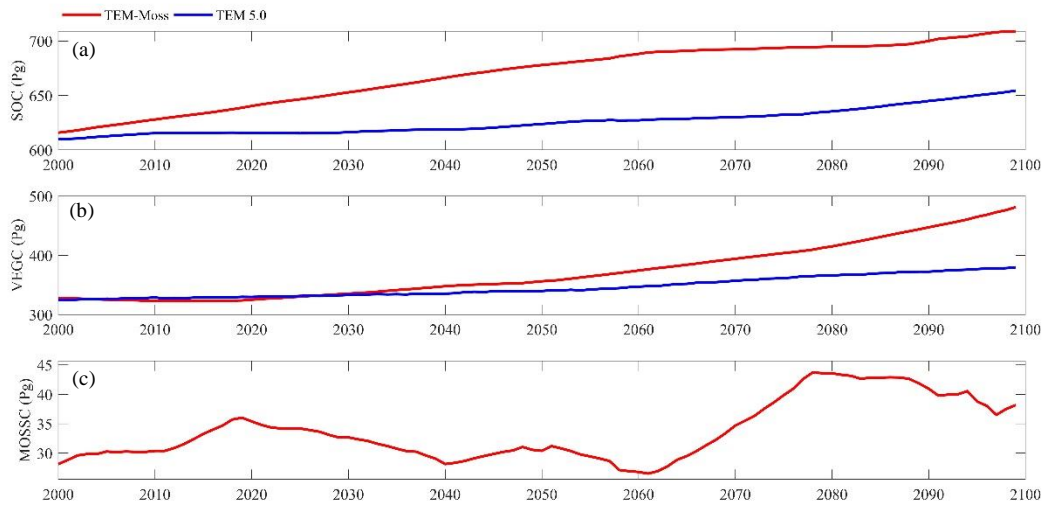
1005 Figure 13. Spatial distribution of NEP simulated for the periods (a) 2000–2050, (b) 2051–2099
1006 by TEM_Moss, and by TEM 5.0 (c, d) during the 21st century under RCP 2.6 scenario (upper
1007 panel) and RCP 8.5 scenario (bottom panel). Positive values of NEP represent sinks of CO₂ into
1008 terrestrial ecosystems, while negative values represent sources of CO₂ to the atmosphere.

1009

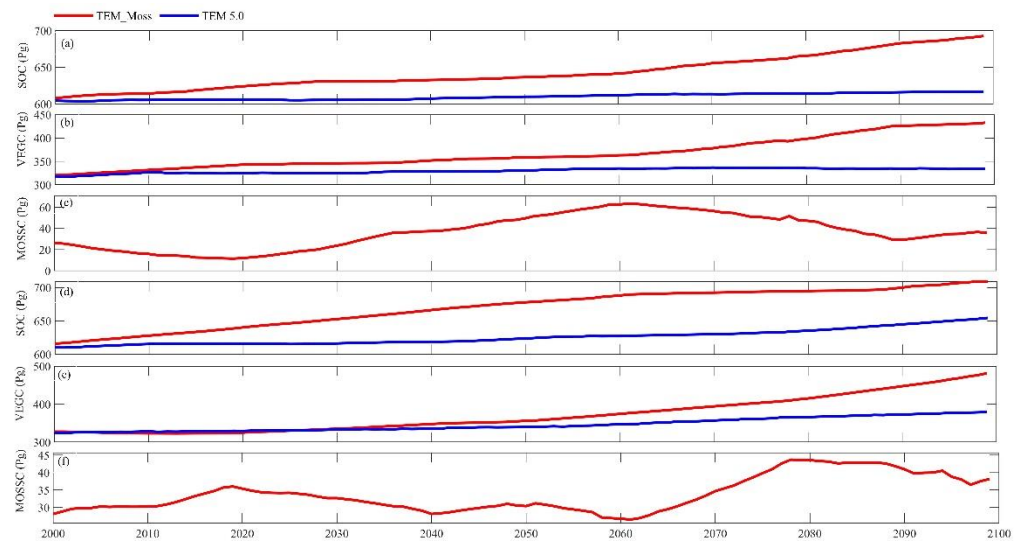
1010



1011

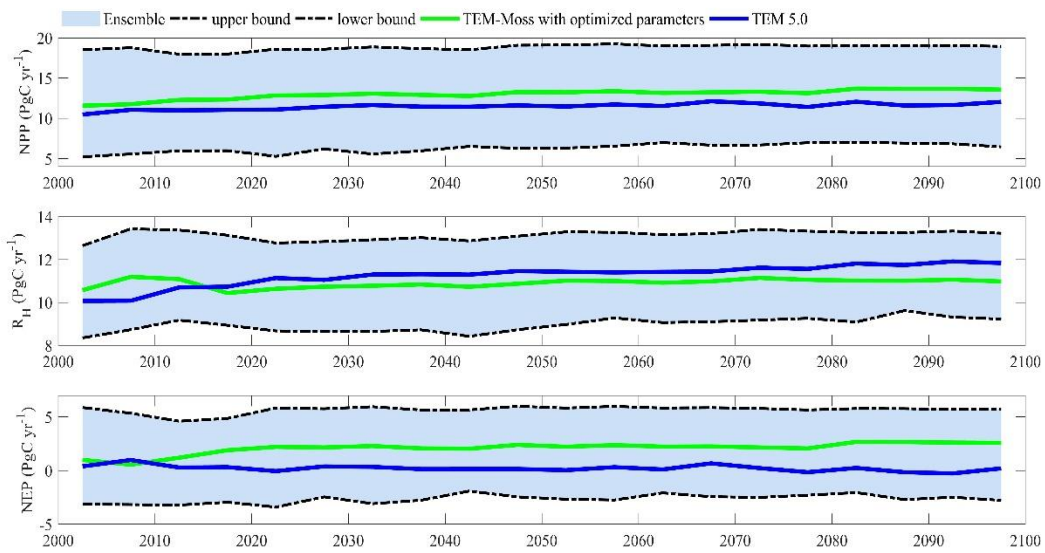


1012

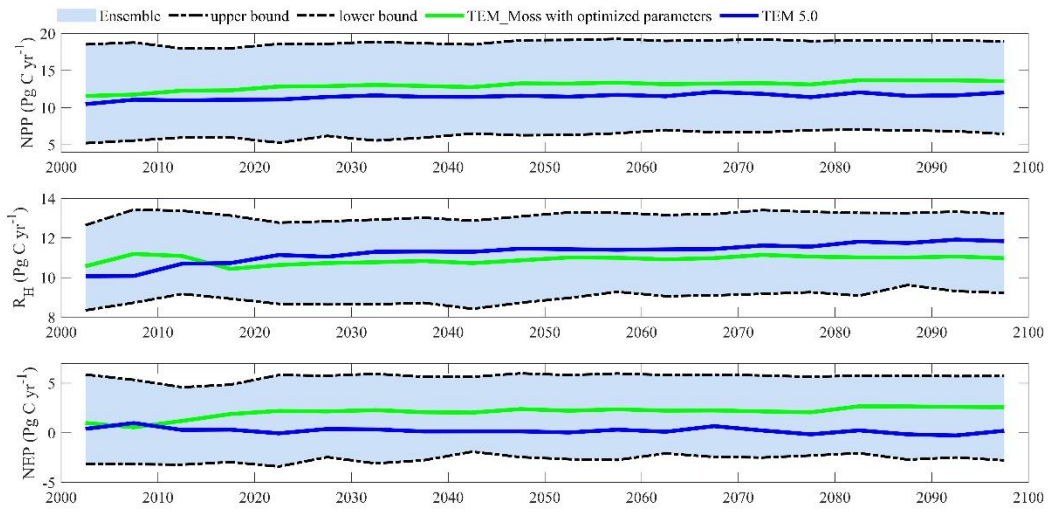


1013 Figure 14. Simulated annual soil organic carbon (SOC, (a, d)a), vegetation carbon (VEGC, (b,
 1014 e)b), and moss carbon (MOSSC, (c, f)e) during the 21st century by TEM_Moss and TEM 5.0
 1015 under RCP 2.6 scenario (a, b, c upper panel) and RCP 8.5 scenario (d, e, f bottom panel).

1016
 1017
 1018
 1019
 1020
 1021
 1022
 1023 (a)

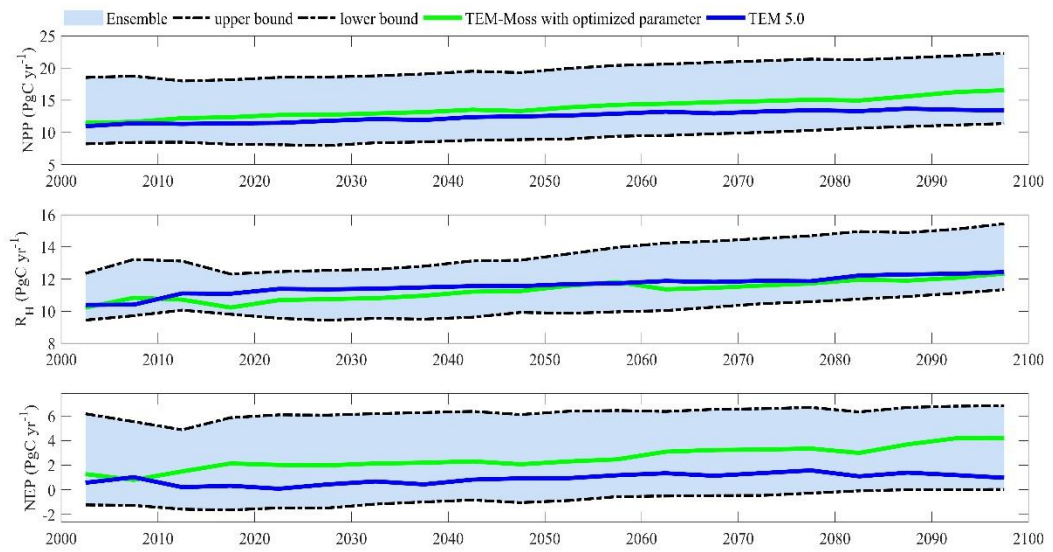


1024

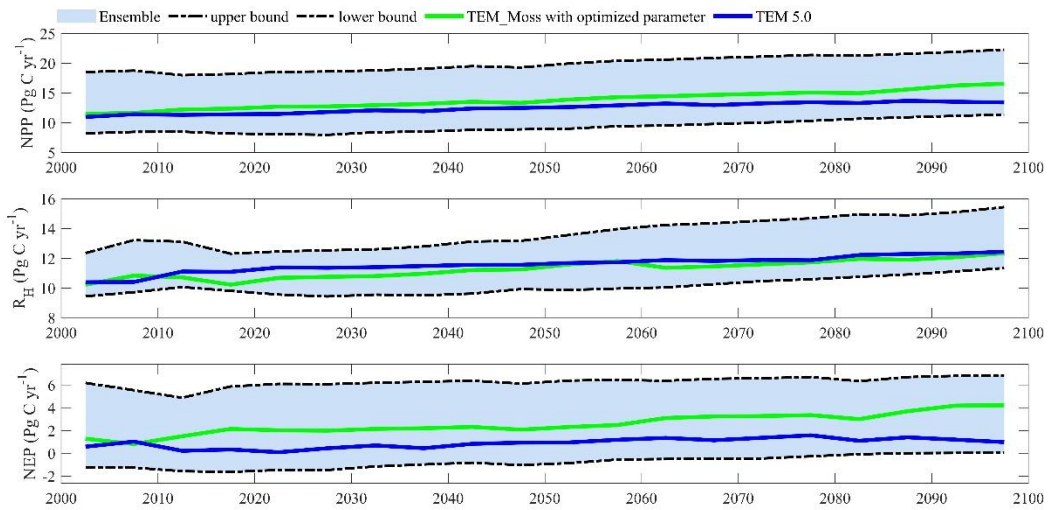


1025

1026 (b)



1027



1028

1029 Figure 15. 5-year moving average plots for carbon fluxes under the (a) RCP 2.6 scenario and (b)
 1030 RCP 8.5 scenario. The blue area represents the upper and lower bounds of simulations.

1031

1032

1033

1034 **Table 1. Parameters associated with moss activities in TEM_Moss**

Parameter	Units	descriptions	Parameter range (value)	references
C_{\max}	g C m^{-2}	maximum rate of C assimilation	[50,500]	Launiainen et al. (2015); Williams &
b	$\mu\text{mol m}^{-2}$	Light half-saturation level	[5, 150]	Launiainen et al. (2015); Raich et al.
T_{\min}	$^{\circ}\text{C}$	minimum temperature	[-10, 10]	Frolking et al. (1996); Raich et al. (1991)
T_{\max}	$^{\circ}\text{C}$	maximum temperature	[30, 80]	Frolking et al. (1996); Raich et al. (1991)
T_{opt}	$^{\circ}\text{C}$	optimal temperature	[15, 30]	Frolking et al. (1996); Raich et al. (1991)
w_{\min}	mm	minimum water content for moss	[0.5, 15]	Frolking et al. (1996); Launiainen et al.
w_{\max}	mm	maximum water content for moss	[150, 380]	Frolking et al. (1996); Launiainen et al.
w_{opt}	mm	optimal water content for moss	[10, 150]	Frolking et al. (1996); Zhuang et al.
k_m	$\mu\text{L/L}$	CO_2 concentration half-saturation level	[50, 500]	Zhuang et al. (2002); Raich et al. (1991)
$R_{10, m}$	g C m^{-2}	moss respiration rate at 10 $^{\circ}\text{C}$	[0,40]	Frolking et al. (1996); Launiainen et al.
$Q_{10, m}$	-	moss respiration temperature sensitivity	[1.5, 2.5]	Frolking et al. (1996); Launiainen et al.
$w_{\text{opt}, r}$	mm	optimal water content for moss	[10, 150]	Frolking et al., 1996; Zhuang et al.
cfall_m	$\text{g}^{-1}\text{g}^{-1} \text{mon}^{-1}$	constant proportion for carbon litterfall	[0.001, 0.01]	Zhuang et al. (2002); Raich et al. (1991)
N_{\max}	gN m^{-2}	maximum rate of N uptake by mosses	[0.1,5]	Zhuang et al. (2002); Raich et al. (1991)
k_n	g m^{-2}	Half-saturation constant for N uptake by	1.0	Zhuang et al. (2002); Raich et al. (1991)
A_m	-	relative allocation of effort to C vs. N	[0,1]	Raich et al. (1991)
w_f	mm	moss field capacity	[10, 80]	Frolking et al. (1996); Raich et al. (1991)
nfall_m	$\text{g}^{-1}\text{g}^{-1} \text{mon}^{-1}$	constant proportion for nitrogen litterfall	[0.001, 0.01]	Zhuang et al. (2002); Raich et al. (1991)
D_m	mm	Moss thickness	[0, 100]	Zhuang et al. (2002)

Table 2. Site description and measured NEP data used to calibrate TEM_Moss

Site Name	Location (Longitude (degrees) /Latitude (degrees))	Elevation (m)	Vegetation type	Description	Data range	Citations
Univ. of Mich. Biological Station	84.71W 45.56 N	234	Temperate deciduous forest	Located within a protected forest owned by the University of Michigan. Mean annual temperature is 5.83° C with mean annual precipitation of 803mm	01/2005- 12/2006	Gough et al. (2013)
Howland Forest (main tower)	68.74W 45.20N	60	Temperate coniferous forest	Closed coniferous forest, minimal disturbance.	01/2004- 12/2004	Davidson et al. (2006)
UCI-1964 burn site	98.38W 55.91N	260	Boreal forest	Located in a continental boreal forest, dominated by black spruce trees, within the BOREAS northern study area in central Manitoba, Canada.	01/2004- 10/2005	Goulden et al. (2006)
KUOM Turfgrass Field	93.19W 45.0N	301	Grassland	A low-maintenance lawn consisting of cool-season turfgrasses.	01/2006- 12/2008	Hiller et al. (2010)
Atqasuk	157.41W 70.47N	15	Wet tundra	100 km south of Barrow, Alaska. Variety of moist-wet coastal sedge tundra, and moist-tussock tundra surfaces in the more well-drained upland.	01/2005- 12/2006	Oechel et al. (2014);
Ivotuk	155.75W 68.49N	568	Alpine tundra	300 km south of Barrow and is located at the foothill of the Brooks Range and is classified as tussock sedge, dwarf-shrub, moss tundra.	01/2004- 12/2004	McEwing et al. (2015)

Table 3. Site description and measured NEP data used to validate TEM_Moss

Site Name	Location (Longitude (degrees) /Latitude (degrees))	Elevation (m)	Vegetation type	Description	Data range	Citations
Bartlett Experimental Forest	71.29W/ 44.06N	272	Temperate deciduous forest	Located within the White Mountains National Forest in north-central New Hampshire, USA, with mean annual temperature of 5.61 °C and mean annual precipitation of 1246mm.	01/2005- 12/2006	Jenkins et al. (2007); Richardson et al. (2007)
Howland Forest (main tower)	68.74W/ 45.20N	60	Temperate coniferous forest	Closed coniferous forest, minimal disturbance.	01/2003- 12/2003	Davidson et al. (2006)
UCI-1964 burn site	98.38W/ 55.91N	260	Boreal forest	Located in a continental boreal forest, dominated by black spruce trees, within the BOREAS northern study area in central Manitoba, Canada.	01/2002- 12/2003	Goulden et al. (2006)
Brookings	96.84W/ 44.35N	510	Grassland	Located in a private pasture, belonging to the Northern Great Plains Rangelands, the grassland is representative of many in the north central United States, with seasonal winter conditions and a wet growing season.	01/2005- 12/2006	Gilmanov et al. (2005)
Atqasuk	157.41W / 70.47N	15	Wet tundra	100 km south of Barrow, Alaska. Variety of moist-wet coastal sedge tundra, and moist-tussock tundra surfaces in the more well-drained upland.	01/2003- 12/2004	Oechel et al. (2014);
Ivotuk	155.75W / 68.49N	568	Alpine tundra	300 km south of Barrow and is located at the foothill of the Brooks Range and is classified as tussock sedge, dwarf-shrub, moss tundra.	01/2005- 12/2005	McEwing et al. (2015)

Table 4. Site description and measured volumetric soil moisture data used to validate TEM_Moss

Site	Location (Longitude (degrees) /Latitude (degrees))	Elevation (m)	Vegetation type	Data range	Citations
US-Ivo	155.75W/ 68.49N	579	Alpine tundra	01/2015- 12/2016	Oechel & Kalhori (2018)
BOREAS NSA-OBS	98.48W/ 55.88N	259	Boreal forest	07/1995- 06/1997	Stangel & Kelly (1999)
NL-Loo	5.74E/ 52.17N	25	Temperate coniferous forest	05/1997- 12/1998	Falge et al. (2005)
DK-Sor	11.64E/ 55.49N	40	Temperate deciduous forest	01/1997- 12/1999	Falge et al. (2005)
US-Bkg	96.84W/ 44.35N	510	Grasslands	01/2005- 12/2006	Gilmanov et al. (2005)
US-Atq	157.41W/ 70.47N	25	Wet tundra	01/2015- 12/2016	Oechel & Kalhori (2018)

Table 5. Site description and measured soil temperature at 5cm depth data used to validate TEM_Moss

Site	Location (Longitude (degrees) /Latitude (degrees))	Elevation (m)	Vegetation type	Data range	Citations
US-Ivo	155.75W/ 68.49N	579	Alpine tundra	01/2015- 12/2016	Oechel & Kalhori (2018)
BOREAS NSA-OBS	98.48W/ 55.88N	259	Boreal forest	01/1995- 12/1998	Stangel & Kelly (1999)
US-Ho1	68.74W/ 45.2N	60	Temperate coniferous forest	01/1996- 12/1997	Falge et al. (2005)
BE-Vie	6.0E/ 50.3N	493	Temperate deciduous forest	01/1997- 12/1998	Falge et al. (2005)
US-Bkg	96.84W/ 44.35N	510	Grasslands	01/2005- 12/2006	Gilmanov et al. (2005)
US-Atq	157.41W/ 70.47N	25	Wet tundra	01/2015- 12/2016	Oechel & Kalhori (2018)

Table 6. Model validation statistics for TEM_Moss and TEM 5.0 at six sites with NEP data

Site Name	Vegetation type	Models	Intercept	Slope	R-square	Adjusted R-square	RMSE	p-value
Ivotuk	Alpine tundra	TEM_Moss	0.46	0.61	0.72	0.70	3.57	<0.001
		TEM 5.0	-0.22	0.75	0.43	0.41	5.88	0.02
UCI-1964 burn site	Boreal forest	TEM_Moss	-0.13	1.01	0.91	0.90	8.33	<0.001
		TEM 5.0	-2.45	1.29	0.75	0.74	20.1	<0.001
Howland Forest (main tower)	Temperate coniferous forest	TEM_Moss	-1.28	1.05	0.83	0.81	19.69	<0.001
		TEM 5.0	-2.22	0.97	0.62	0.61	31.23	0.002
Bartlett Experimental Forest	Temperate deciduous forest	TEM_Moss	-0.49	1.03	0.94	0.94	19.06	<0.001
		TEM 5.0	-2.49	1.04	0.91	0.89	23	<0.001
Brookings	Grassland	TEM_Moss	0.36	1.02	0.85	0.84	8.95	<0.001
		TEM 5.0	2.58	0.75	0.62	0.6	13.07	<0.001
Atqasuk	Wet tundra	TEM_Moss	-0.36	0.97	0.84	0.83	5.13	<0.001
		TEM 5.0	1.99	0.75	0.75	0.74	6.56	<0.001

Table 7. Model validation statistics for TEM_Moss and TEM 5.0 at six sites with volumetric soil moisture data

Site ID	Vegetation type	Models	Intercept	Slope	R-square	Adjusted R-square	RMSE	p-value
US-Ivo	Alpine tundra	TEM_Moss	8.56	0.34	0.74	0.72	20.8	<0.001
		TEM 5.0	10.67	0.29	0.64	0.62	21.76	<0.001
BOREAS NSA-OBS	Boreal forest	TEM_Moss	10.71	0.51	0.52	0.51	11.1	<0.001
		TEM 5.0	16.47	0.43	0.32	0.31	11.96	<0.001
NL-Loo	Temperate coniferous forest	TEM_Moss	0.47	0.82	0.83	0.81	4.0	<0.001
		TEM 5.0	3.75	0.72	0.49	0.48	4.5	<0.001
DK-Sor	Temperate deciduous forest	TEM_Moss	1.39	0.86	0.67	0.65	3.65	<0.001
		TEM 5.0	10.41	0.54	0.4	0.39	4.06	<0.001
US-Bkg	Grassland	TEM_Moss	5.64	0.8	0.51	0.49	6.05	<0.001
		TEM 5.0	22.24	0.41	0.21	0.2	7.34	0.027
US-Atq	Wet tundra	TEM_Moss	7.76	0.77	0.87	0.85	7.38	<0.001
		TEM 5.0	6.74	0.68	0.85	0.84	7.63	<0.001

Table 8. Model validation statistics for TEM_Moss and TEM 5.0 at six sites with soil temperature at 5cm depth data

Site ID	Vegetation type	Models	Intercept	Slope	R-square	Adjusted R-square	RMSE	p-value
US-Ivo	Alpine tundra	TEM_Moss	-0.34	1.16	0.83	0.82	2.54	<0.001
		TEM 5.0	0.54	1.36	0.75	0.73	3.94	<0.001
BOREAS NSA-OBS	Boreal forest	TEM_Moss	-0.05	0.91	0.9	0.88	2.24	<0.001
		TEM 5.0	0.27	0.81	0.84	0.82	2.9	<0.001
US-Ho1	Temperate coniferous forest	TEM_Moss	0.7	0.95	0.81	0.79	2.93	<0.001
		TEM 5.0	-0.06	0.99	0.77	0.76	3.41	<0.001
BE-Vie	Temperate deciduous forest	TEM_Moss	0.57	0.92	0.83	0.81	1.82	<0.001
		TEM 5.0	1.88	0.85	0.69	0.68	2.56	<0.001
US-Bkg	Grassland	TEM_Moss	0.17	0.87	0.91	0.89	2.87	<0.001
		TEM 5.0	-0.01	0.91	0.89	0.87	3.04	<0.001
US-Atq	Wet tundra	TEM_Moss	1.36	0.86	0.84	0.82	3.63	<0.001
		TEM 5.0	4.33	0.99	0.75	0.74	6.17	<0.001

Table 9. Average annual NPP, R_H and NEP (as Pg C per year) during the 20th century estimated by two models.

Average annual carbon fluxes (Pg_C yr ⁻¹)		TEM_Moss	TEM 5.0	Difference	Moss NPP/ Vascular plants NPP
NPP	Moss NPP	1.69	-	-	21.3%
	Vascular plants NPP	7.93	8.8	-	
	Total NPP	9.6	8.8	0.8	
R _H		7.38	7.91	-0.53	
NEP		2.22	0.89	1.33	

Table 10. Increasing of SOC, vegetation carbon (VGC), and moss carbon (MOSSC) from 1900 to 2000, and total carbon storage during the 20th century predicted by two models.

Models	Carbon pools	Carbon pool amounts in 1900/2000 (units: Pg)	Changes in carbon pools during the 20 th century (units: Pg)
TEM_Moss	SOC	587.1/683.4	96.3
	VEGC	297.5/412.7	115.2
	MOSSC	19.6/30	10.4
	Total	904.2/1126.1	221.9
TEM 5.0	SOC	583.2/614.9	31.7
	VEGC	291.1/348.6	57.5
	Total	874.3/963.5	89.2

Table 11. Average annual NPP, R_H and NEP (as Pg C per year) during the 21st century estimated by two models under (a) RCP 8.5 scenario and (b) RCP 2.6 scenario.

(a)

Average annual carbon fluxes (Pg_C yr ⁻¹)		TEM_Moss	TEM 5.0	Difference	Moss NPP/ Vascular plants NPP
NPP	Moss NPP	3.84	-	-	38.4%
	Vascular plants NPP	10	12.53	-	
	Total NPP	13.84	12.53	1.31	
R _H		11.28	11.54	-0.21	
NEP		2.56	0.99	1.57	

(b)

Average annual carbon fluxes (Pg_C yr ⁻¹)		TEM_Moss	TEM 5.0	Difference	Moss NPP/ Vascular plants NPP
NPP	Moss NPP	3.74	-	-	40.5%
	Vascular plants NPP	9.24	11.52	-	
	Total NPP	12.98	11.52	1.46	
R _H		10.91	11.24	-0.33	
NEP		2.07	0.28	1.79	

Table 12. Increasing of SOC, vegetation carbon (VGC), and moss carbon (MOSSC) from 1900 to 2000, and total carbon storage during the 21st century predicted by two models under (a) RCP 2.6 scenario and (b) RCP 8.5 scenario.

(a)

Models	Carbon pools	Carbon pool amounts in 2000/2099 (units: Pg)	Changes in carbon pools during the 21 st century (units: Pg)
TEM_Moss	SOC	608.1/692.8	84.7
	VEGC	320.2/432.8	112.6
	MOSSC	26.2/35.6	9.4
	Total	954.5/1161.2	206.7
TEM 5.0	SOC	604.4/616.5	12.1
	VEGC	318.2/333.7	15.5
	Total	922.6/950.2	27.6

(b)

Models	Carbon pools	Carbon pool amounts in 2000/2099 (units: Pg)	Changes in carbon pools during the 21 st century (units: Pg)
TEM_Moss	SOC	615.9/708.4	92.5
	VEGC	327.8/481.4	153.6
	MOSSC	28.1/38.2	10.1
	Total	971.8/1228.0	256.2
TEM 5.0	SOC	610.2/654.4	44.2
	VEGC	324.9/379.4	54.5
	Total	935.1/1033.8	98.7